INFLUENCE OF DISPERSION, EXCLUSION, AND METATHETICAL SORPTION ON THE TRANSPORT OF INORGANIC SOLUTES IN A CALCIUM-SATURATED POROUS MEDIUM

By

NARAINE PERSAUD

A DISSERTATION PRESENTED TO THE GRADUATE COUNCIL OF
THE UNIVERSITY OF FLORIDA
IN PARTIAL FULFILLMENT OF THE REQUIREMENTS FOR THE
DEGREE OF DOCTOR OF PHILOSOPHY

UNIVERSITY OF FLORIDA

1978

To my Parents

ACKNOWLEDGEMENTS

The author wishes to express his sincere gratitude to Dr. J. M. Davidson, chairperson of his supervisory committee, for the unique and conscientious guidance and help provided throughout the duration of this study.

The helpful suggestions made by members of the committee, viz. Dr. J. G. A. Fiskell, Dr. L. Hammond and Dr. S. J. Locascio, during their review of this manuscript are highly appreciated. The interest shown by Dr. R. S. Mansell who was also a member of the committee until he left on sabbatical leave is also highly esteemed.

A special word of thanks is reserved for Dr. P. S. C. Rao and Mr. Ron Jessup for the useful advice given during many discussions on diverse subjects pertinent to this study.

The cheerful companionship of Mr. Rick Janka did much to relieve the tedium of the long hours spent in the laboratory.

The financial assistance provided by the Soil Science Department is gratefully acknowledged.

Superlatives fail to express the author's deep feelings towards his wife Savi whose constant encouragement and support were sin qua non to the successful completion of this study.

TABLE OF CONTENTS

CHAPTER

LIST OF FIGURES

LIST OF FIGURES (continued)

Abstract of Dissertation Presented to the Graduate Council
of the University of Florida in Partial Fulfillment
of the Requirements for the Degree of Doctor of Philosophy

INFLUENCE OF DISPERSION, EXCLUSION, AND METATHETICAL SORPTION ON THE TRANSPORT OF INORGANIC SOLUTES IN A CALCIUM-SATURATED POROUS MEDIUM

By

Naraine Persaud

June 1978

Chairperson: J. M. Davidson
Major Department: Soil Science

Classical thermodynamic concepts were used to derive general relationships to describe the equilibrium disposition of charged species in aqueous contact with a cation exchanger. It was shown through these relationships that anions would be excluded by the exchanger and solution phase cations of the same type as those initially saturating the exchanger influenced the adsorption of counterions. The latter result was verified with exchange adsorption isotherms for Na^+ and Li^+ in solutions of 0.05 M, 0.02 M, and 0.005 M $Ca(NO_3)_2$ and a Ca-saturated exchanger. These results illustrated that Na^+ and Li^+ adsorption decreased with increasing concentrations of Ca^{2+} in the equilibrium solution. Similar results were observed for the adsorption of $^{45}Ca^{2+}$ in solutions of 0.075 M and 0.05 M $Ca(NO_3)_2$. The adsorption isotherms were linear over the range of concentrations studied for a given $Ca(NO_3)_2$

concentration. The thermodynamic relations in conjunction with the Debye-Hückel theory were used to predict the slopes for these isotherms. The computed values agreed reasonably well with their experimental counterparts. These results demonstrated inductively, that electrostatic ion-ion interactions as conceived and quantified by the Debye-Hückel theory, constituted the physical basis for the observed equilibrium behaviour.

The consequences of the foregoing results on the transport behaviour of Na^+, Li^+, $^{45}Ca^{2+}$ and Cl^- were investigated using miscible displacement experiments in laboratory columns packed with the exchanger material. These studies were conducted using pulse inputs of tracer solutions containing various concentrations of $Ca(NO_3)_2$. Tritiated water (HTO) was introduced with all tracer pulses to evaluate hydrodynamic dispersion. An analytical solution to the convective-dispersion mass transport equation for a reactive solute (linear adsorption isotherm) was used to describe the experimental data.

As expected, the elution curves for Cl^- were displaced to the left of those for HTO illustrating exclusion of Cl^- by the exchanger. The elution curves for Na^+, Li^+ and $^{45}Ca^{2+}$ were displaced to the right of those for HTO, the shift increasing with decreasing concentration of Ca^{2+} in the tracer solution. Anomalous and unusual patterns were observed in some of the elution curves. The elution curves for Na^+ in 0.005 M $Ca(NO_3)_2$ and for $^{45}Ca^{2+}$ in 0.05 M $Ca(NO_3)_2$ showed deviations that simulated the effect of kinetic mass transfer processes. Inflections were observed on the desorption side of the pulse elution data for Li^+ in 0.02 M and 0.005 M $Ca(NO_3)_2$ and for $^{45}Ca^{2+}$ in 0.075 M $Ca(NO_3)_2$. These elution curves were not described by the analytical

solution. Further experimentation demonstrated that these data could be explained on the basis of differences between the parameters characterizing exchange adsorption and desorption. A quantitative treatment, based on the thermodynamic relations coupled with the Debye-Huckel theory, showed that these differences were a direct consequence of the metathetical nature of the sorption process.

Some cursory observations were made regarding the transport behavior of Na^+, HTO and Cl^- under steady-state unsaturated water flow conditions. The exclusion of Cl^- was again evident. Discrepancies between the experimental and analytical curves for Na^+ indicated that portions of the water-unsaturated exchanger phase became either inaccessible to Na^+ or was accessible only by diffusion.

INTRODUCTION

The classic work of Thompson and Way, reported during 1850-1852 on exchange reactions involving soil materials treated with inorganic salt solutions, marked the beginning of systematic investigations of ion exchange. Their experiments were conducted decades before Arrenhius proposed the theory of electrolytic dissociation and many years before the law of mass action was enunciated. There was, therefore, no existing theoretical framework within which the two English agricultural chemists could interpret their observations. The principle that substances did not react except in a dissolved state was generally accepted by chemists of their era. Whether the reactions reported were purely chemical or physical became a debated question. This dichotomy in views has still not been fully resolved.

For a period after its discovery, ion exchange remained of academic interest until about 1907 when it was used to soften water. Instability under non-neutral pH conditions and the low capacity of the available natural and artificial siliceous ion exchangers provided the impetus for the discovery and synthesis of organic ion exchangers. These synthetic materials are now utilized in most industrial and laboratory applications involving ion exchange. Extensive research concurrent with their increasingly widespread use has resulted in the evolution of more comprehensive and refined ion exchange theories.

The miscible displacement technique has in the past few decades become an increasingly valuable experimental tool for studying

physico-chemical processes associated with solute transport in porous media. Theoretical concepts on physico-chemical interactions of particular solutes have been successfully incorporated into classical mass transport models. Comparisons between experimental and theoretical results on solute transport have served to verify concepts and to evaluate the influence of physical factors. The diversity of possible physico-chemical interactions of inorganic ions with various soil components makes natural soil materials a complex medium in which to study ion exchange. This difficulty can be circumvented somewhat by the use of synthetic exchangers.

The primary objective of this study was to evaluate some theoretical concepts on ion exchange equilibria and kinetics using the miscible displacement technique and a porous medium prepared from a synthetic organic ion exchanger.

CHAPTER 1

A REVIEW OF PERTINENT CONCEPTS ON SOLUTE TRANSPORT DURING MISCIBLE DISPLACEMENT IN DISCRETE POROUS MEDIA AND ON INORGANIC ION EXCHANGE EQUILIBRIA AND KINETICS

Miscible Displacement Processes in Discrete Porous Media

Miscible displacement is the term used to describe a process whereby one fluid is displaced by another, both fluids being miscible in each other. This process occurs in a soil when a solution is displaced downwards by incoming rain or irrigation water or when sea water displaces fresh water during drawdown in coastal aquifers. In the petroleum industry, fluids miscible with crude oil are used to increase the efficiency with which the crude oil is displaced from oil bearing strata during secondary operations. Separation and recovery processes in industrial packed towers or in chromatographic columns are other examples of miscible displacement processes in porous media.

The transport behavior of materials dissolved in the displacing or displaced fluids is influenced by the physical properties of the medium (particle size, shape, and manner of packing), rheological properties of the fluids, and both the equilibria and rates of reactions between the solute and solid matrix of the porous medium. Miscible displacement experiments where there is no interaction between the medium and the solute can be used to evaluate the effect of the first two factors. The combined effect of the first two factors has been grouped under the term "dispersion" and a considerable body of literature

has grown out of these studies. Excellent reviews on dispersion have been presented by Fried and Combarnous (25) and Bear (6).

Dispersion of Solutes During Miscible Displacement in Discrete Porous Media

Dispersion is the result of a physical mixing between displacing and displaced fluids. Its effect can be studied by measuring the relative concentration gradients between the displacing and displaced fluids. Gradients are usually determined experimentally by withdrawing samples at suitable time intervals at a fixed location in the flow region under consideration. This technique and the relative concentration versus time plots, termed breakthrough curves, have been described by Nielsen and Biggar (53).

Dispersion in many practical situations involving solute transport, especially in chromatographic and industrial separations, has provided much of the initial motivation to quantify and describe the process. Several theoretical approaches have been taken in this connection. Attempts have been made to predict macroscopic dispersion effects based on various geometrical models of the microstructure of the channels in the porous matrix (23,33,64). These, however, require complex mathematical analyses, are rather academic in nature, and have not proven to be useful. Limitations of this approach have been discussed by Scheidegger (66). Analysis of solute transport based on a physical description of the flow region into theoretical plates has proved quite useful in evaluating dispersion in chromatographic separations (28,68).

An approach based on differential mass-balance equations for the solute in the fluid flow field has been successful and has gained wide

acceptance. Taylor (67) used this approach to study solute dispersion during laminar flow in straight capillary tubes. Analysis of the differential mass-balance equation with appropriate initial and boundary conditions yielded expressions which satisfactorily explained his experimental results. These results showed that dispersion was dependent on the fluid velocity and the distance travelled by the displacing front. During laminar flow of Newtonian fluids in straight tubes, a typical parabolic velocity distribution is produced. This would not be the case for a discrete porous medium with geometrically complex, tortuous channels between the particles. For a porous medium it is assumed that the microscopic velocities between particles would fluctuate continuously in a random manner about some mean value. This viewpoint led to a concept that was developed almost simultaneously by Scheidegger (65) and Danckwerts (16). Although they used somewhat different approaches in their arguments, they agreed that dispersion could be regarded as a quasi-diffusion process. With this concept, the classical differential equation for mass transport by simultaneous convection and diffusion could be applied if an appropriate change was made in the physical meaning attached to the diffusion coefficient. The validity of this approach was demonstrated immediately by other investigators (4,19,52).

The Convective-Dispersion Equation Including Assumptions, Auxiliary Conditions, Analysis, and Limitations

Mass balance considerations for transport by simultaneous diffusion and convection in a homogenous, isotropic porous medium yield the classical convective-diffusion equation. In one-dimension this equation (39) is

$$\frac{\partial C}{\partial t} = \frac{\partial}{\partial x}\{D \frac{\partial C}{\partial x} - \underline{v}C\} \quad (1)$$

where, $C(x,t)$ is concentration of solute in the fluid of the flow region (M/L^3), t is time (T), x is distance (L), D is the diffusion coefficient (L^2/T), and $\underline{v}$ is vector velocity of the fluid at any point in the flow region (L/T).

Because of the pore size distribution, complex fluid velocity fields arise within the channels of the porous medium. It is assumed, however, that these velocity vectors are statistically distributed about some fixed mean velocity vector $\underline{v}^*$. The probability distribution of the deviations about this average is then considered by the introduction of a quasi-diffusion coefficient, D^*, which characterizes the unidirectional transport of the solute. This quasi-diffusion coefficient has been termed the "dispersion coefficient" by Scheidegger (65). If it is also assumed that the dispersion coefficient is independent of concentration, then equation (1) reduces to

$$\frac{\partial C}{\partial t} = D^*\frac{\partial^2 C}{\partial x^2} - \underline{v}^*\frac{\partial C}{\partial x} \quad (2)$$

As shown by Scheidegger (65) and in a somewhat more heuristic manner by Rifai et al. (59), this equation can also be obtained by arguments based entirely on probability calculus. This equation has been appropriately called the "convective-dispersion" equation.

It is at once apparent from its description that $\underline{v}^*$ is the experimentally measurable average pore-water velocity of the fluid in the porous medium. This is given by the relationship

$$\underline{v}^* = \frac{Q}{\theta_v A t} \tag{3}$$

where, Q is volume of fluid introduced (L^3), A is the cross sectional area of the flow region (L^2), θ_v is the fractional fluid filled porosity of the medium (L^3/L^3), and t is time (T).

It is also clear that D is related to D* in the following manner:

$$D^* \geq D, \qquad \lim_{\underline{v}^* \to 0} D^* = D. \tag{4}$$

For a fixed X = L, the solution of the convective-dispersion equation would be C = C(t, D*, L, v*) where D*, L, and v* are parameters. It is advantageous to formulate the differential equation and auxiliary conditions in dimensionless form. The problem then becomes independent of units and the parameters are reduced to dimensionless groupings. In addition, interactions among the parameters become more obvious. The dimensionless variables are $C^* = \frac{C}{Co}$, $X = \frac{x}{L}$, and $T = \frac{v^* t}{L}$ which, when substituted into equation (2) give

$$\frac{\partial C^*}{\partial T} = \frac{D^*}{v^* L} \frac{\partial^2 C^*}{\partial X^2} - \frac{\partial C^*}{\partial X}. \tag{5}$$

The reciprocal of the dimensionless grouping $\frac{D^*}{v^* L}$ has been termed the Peclet number, usually denoted by P, and appears as a single parameter in solutions of the transformed equation. The dimensionless time T corresponds physically to the number of fluid-filled void volumes introduced into the flow region.

The convective-dispersion equation in either form [equation (2) or (5)] has been analyzed for various sets of boundary and initial conditions appropriate to different physical situations. These have been summarized by Nir and Gershon (54). The analyses are based on the theory of equations in partial derivatives, a very difficult

and still incomplete branch of higher mathematics. Analytical solutions can be obtained with comparative ease for simple sets of boundary and initial conditions; however, for complex conditions or for finite domains of definition, one is forced to resort to numerical integration methods.

Analytic solutions to equation (2) have been obtained for two simple sets of conditions. These can be written as

$$\text{I.}\quad C(x > 0,\ t = 0) = 0 \quad , \quad C(x = 0,\ t > 0) = Co,$$
$$C(x = \infty,\ t > 0) = 0 \tag{6}$$

$$\text{II.}\quad C(x > 0,\ t = 0) = 0 \quad , \quad C(x = 0,\ 0 < t \leq t_1) = Co$$
$$C(x = 0,\ t > t_1) = 0 \quad , \quad C(x = \infty,\ t > 0) = 0 \tag{7}$$

Physically, the first set of conditions corresponds to a solute of concentration Co continuously displacing the solvent in a semi-infinite medium. In the second case, the same displacement is allowed to proceed for a time t_1 and for all times thereafter the displacing solution is replaced by pure solvent. These two situations have been termed miscible displacement with a "step input" and "pulse input," respectively.

The solution to equation (2) for a "step input" (59) is given by

$$\frac{C(x,t)}{Co} = \frac{1}{2}\{\operatorname{erfc}[\frac{x-vt}{2\sqrt{Dt}}] + \exp(\frac{vx}{D})\ \operatorname{erfc}[\frac{x+vt}{2\sqrt{Dt}}]\} \tag{8}$$

where the superscripts have been omitted from D^* and v^*.

Except near the inlet (x = 0) or for very small times, unless D is large, the second term in equation (8) is small and can be neglected. Applying this condition and the identity erfc(x) = 1- erf(x), equation (8) reduces to

$$\frac{C(x,t)}{Co} = \frac{1}{2}\{1 - \text{erf}[\frac{x-vt}{2\sqrt{Dt}}]\} \qquad (9)$$

The cumulative distribution function P(x) for a standardized Gaussian random variable of mean $\bar{x}$ and standard deviation σ is given by

$$P(x) = \frac{1}{2}\{1 + \text{erf}[\frac{x-\bar{x}}{\sqrt{2}\sigma^2}]\} \; . \qquad (10)$$

From the identity erf(-x) = -erf(x), it is apparent that equation (9) represents, for a given value of x = L, a Gaussian cumulative distribution function of mean L and standard deviation $\sqrt{2Dt}$.

The solution for the "pulse input" is obtained by shifting the solution for the "step input" by the time width of the pulse and subtracting this from the original solution. Applying this rather intuitive procedure to equation (9) gives

$$\frac{C(x,t)}{Co} = \frac{1}{2}\{\text{erf}[\frac{x-v(t-t_1)}{2\sqrt{D(t-t_1)}}]-U(t-t_1)\text{erf}[\frac{x-vt}{2\sqrt{Dt}}]\} \qquad (11)$$

where $U(t-t_1)$ is the Heaviside unit function.

The previous equations have been used to analyze experimental results from finite laboratory columns. As shown by Nir and Gershon (54) only a small error is involved by assuming a finite rather than a semi-infinite column.

The boundary conditions appropriate for a defined finite domain are obtained by imposing the conservation of mass on the fluxes at the boundaries. This results in the following boundary conditions for a step input and a space domain of definition $0 \leq x \leq L$

$$x = 0;\ t > 0; \quad vCo = vC\big|_{x=0} - D\frac{\partial C}{\partial x}\Big|_{x=0} \qquad (12a)$$

$$x = L;\ t > 0; \quad vCe = vC\big|_{x=L} - D\frac{\partial C}{\partial x}\Big|_{x=L} \qquad (12b)$$

where Ce is the exit concentration at a given time.

However, as argued by Danckwerts (16), if at $x = L$, $\left.\frac{\partial C}{\partial x}\right|_{x=L} < 0$ then $C\Big|_{x=L} < C\Big|_{x<L}$. A similar argument holds if at $x = L$, $\left.\frac{\partial C}{\partial x}\right|_{x=L} > 0$. Hence $\left.\frac{\partial C}{\partial x}\right|_{x=L}$ must be equal to zero otherwise a maximum or a minimum exists in the interior of the column. The appropriate condition at $x = L$ must therefore be $\left.\frac{\partial C}{\partial x}\right|_{x=L} = 0$.

An approximate solution to the convective-dispersion equation in dimensionless form for the above boundary conditions has been presented by Brenner (14). In dimensionless form these conditions become

$$X = 0; \quad T > 0; \quad C^* - \frac{1}{P}\frac{\partial C^*}{\partial X} = 1 \tag{13a}$$

$$X = 1; \quad T > 0; \quad \frac{\partial C^*}{\partial X} = 0 \tag{13b}$$

Wehner and Wilhelm (75) and Lindstrom et al. (46) have shown that, for large values of P, the condition at $x = 0$ reduces to $C^* = 1$ for $t > 0$.

In order to make the condition at $x = 0$ homogeneous, Brenner defines $C^* = \frac{C-Co}{C_i-Co}$ where C_i is the initial concentration in the fluid at $t = 0$. The initial concentration was taken to be zero for his solution. Brenner tabulated numerical values of his solution for a wide range of values of P/4. It was found that, with increasing values of P, his solution asymptotically approached the simplified solution given by equation (9). He also discusses the limiting behavior of his solution for $P = 0$ and $P = \infty$. These correspond physically to complete instantaneous mixing and to no dispersion, respectively. His solution has been used frequently for analysis of experimental data from miscible displacement experiments (61).

Numerical procedures for integration of the convective-dispersion equation are all based on methods whereby continuous systems are mathematically reduced to equivalent discrete systems. Suitable algo-

rithms can then be developed and solved iteratively using high speed computers. Serious and difficult mathematical questions of adequacy, accuracy, convergence and stability arise for numerical solutions and adequate answers are often not available. Procedures based on finite differences and finite elements are discussed by Ames (1) and Pinder and Gray (55).

From the assumptions used in its development, the convective-dispersion equation represents an idealized conception of the miscible displacement process. Its shortcomings were demonstrated early by its inability to describe non-reactive solute behavior in unsaturated porous media (53). Also, it fails to predict the effects of density differences between displacing and displaced fluids (62). Its major weakness probably lies in the assumption of a fluid continuum. The presence of dead-end pores and regions where the fluid is hydrodynamically immobile would clearly lead to unpredicted results. Refinements made to handle such cases (15,69) have resulted in better agreement between predicted and experimental results.

Extension of the Continuum Mass Balance Approach for Single Interacting Solutes

The convective-dispersion equation can be extended to describe the transport of a single interacting solute through a porous medium. This requires additional terms to cover the time rate of change of solute concentration in the fluid as a result of mass transfer between the fluid and solid matrix of the medium. For a general case, these terms constitute the difference between the instantaneous adsorption and desorption rates. Equivalently and more conveniently, this

can be expressed in terms of the instantaneous net time rate of accumulation of the solute on the particles of the medium. The concentration of the solute in the matrix expressed as mass of solute/unit mass of matrix can be denoted by $S(x,t)$. The instantaneous net time rate of change of concentration in the fluid due to mass transfer is then $\frac{\rho}{\theta_v}\frac{\partial S}{\partial t}$ in which ρ is the dry bulk density of the matrix and θ_v is the fractional water-filled porosity. Considering only one mass transfer process, the resulting differential equation is

$$\frac{\partial C}{\partial t} = D^*\frac{\partial^2 C}{\partial x^2} - v^*\frac{\partial C}{\partial x} - \frac{\rho}{\theta_v}\frac{\partial S}{\partial t} \qquad (14)$$

The functional form of $S(x,t)$ has profound consequences on the analysis of the resulting differential equation. In general, the mass transfer processes may involve purely diffusion kinetics, irreversible and reversible chemical kinetics or both. Hence, it would be expected that in the general case

$$\frac{\partial S}{\partial t} = f[C, S, \tau, (\lambda_1, \lambda_2 \cdots \lambda_n)_{diffusion}, (\lambda_1, \lambda_2 \cdots \lambda_n)_{chemical}] \qquad (15)$$

where τ is temperature, and $\lambda_1 \cdots \lambda_n$ are parameters characterizing diffusion and chemical kinetics (57). The case of mass transfer involving only irreversible chemical kinetics has been analyzed by Amundson (2).

Processes involving only reversible chemical kinetics can be represented in the general case as

$$\frac{\partial S}{\partial t} = \lambda_1 f_1(S, C, \tau) - \lambda_2 f_2(S, C, \tau) \qquad (16)$$

where λ_1 and λ_2 are constants characterizing the kinetics of sorption and desorption, respectively.

An important simplification of chemical kinetics is based on the assumption that, at a constant temperature, the processes occur fast enough to insure that equilibrium is instantaneous. The functional form of $S(x,t)$ is then given by an equation which describes the equilibrium isotherm. This equation can be experimentally determined or deduced from kinetic equations, if these are known, by setting $\frac{\partial S}{\partial t} = 0$. In general, these isotherms can be represented as

$$S = f(C, \lambda_1 \ldots \lambda_n) \tag{17}$$

where $\lambda_1 \ldots \lambda_n$ are parameters characterizing the equilibrium distribution of the solute between the fluid and solid matrix of the medium.

With this assumption, introducing $\frac{\partial S}{\partial t} = \frac{\partial S}{\partial t} \circ \frac{\partial C}{\partial t}$ in the differential equation gives

$$\frac{\partial C}{\partial t} = \frac{D^*}{R} \frac{\partial^2 C}{\partial x^2} - \frac{v^*}{R} \frac{\partial C}{\partial x} \tag{18}$$

where, $R = 1 + \frac{\rho}{\theta_v} \cdot \frac{\partial S}{\partial C}$

From this equation, some useful deductions can be made regarding the transport behavior of the solute for certain generalized functional forms for the isotherm.

In the case where the isotherm is a single-valued concave downward function $\left.\frac{\partial S}{\partial c}\right|_{c_1} > \left.\frac{\partial S}{\partial c}\right|_{c_2}$ and thus $\left.\frac{v^*}{R}\right|_{c_1} < \left.\frac{v^*}{R}\right|_{c_2}$ for $C_1 < C_2$. Similarly the reverse is true for $C_1 < C_2$ when an adsorption isotherm is represented by a concave upward function. For a linear isotherm, $\frac{v^*}{R}$ is independent of C. Typically, for a pulse input of a non-reactive solute, dispersion causes the elution curves to have a gradual increase in concentration from zero to a maximum on the front and falling again to zero on the back side of the elution data. For a concave downward

isotherm, the concentration effect on the velocity would result in a nullification of dispersion on the front and an enhancement on the back side of the elution curve. This effect would not appear in the case of a linear isotherm and the reverse would be true for a concave upward isotherm. For a linear isotherm, the front and rear of the elution curve would match exactly, but will not match for non-linear isotherms. If the assumption of instantaneous equilibrium was valid for a particular situation, the shape of the elution curve can provide a valuable indication of the type of adsorption isotherm involved in the displacement process. These arguments have been confirmed by analysis of the differential equation for various functional forms of the isotherm, including cases where it was not single-valued (45, 46,70).

As would be expected, the assumption of instantaneous equilibrium is not valid for all situations. Exact solutions of the differential equation incorporating two important models of reversible chemical kinetics have been presented by Amundson(3). These models are

$$\frac{\partial S}{\partial t} = k_1 C - k_2 S \tag{19}$$

for linear adsorption kinetics, and

$$\frac{\partial S}{\partial t} = k_1 C(S_{max} - S) - k_2 S \tag{20}$$

for "Langmuir" kinetics, where S_{max} is the saturation capacity. Numerical procedures have increased the range of possible theoretical models that can be used.

Except for a few cases (24, 69), less effort has been devoted to studying diffusion kinetics. In soils, however, where particles

exist as aggregates and dead end pores are present, diffusion kinetics may be important (69).

Investigation of the simultaneous transport of a number of solutes which influence the mass transfer processes of each other have not been attempted. In addition, comprehensive reviews have not been made of the various equilibrium and kinetic models commonly used by investigators. The equations derived from theory reflect the effects of only those interactions for which the models have been developed. Different theories may well attribute experimental results to quite different causes. This constitutes the deficiency in many studies since it is often extremely difficult if not impossible to independently measure the theoretical parameters introduced in sorption kinetic models.

Equilibria and Kinetics of Inorganic Ion Exchange Adsorption

Inorganic ion exchange was discovered more than a century ago. For soils, ion-exchange properties were traced to their aluminosilicate fractions (73,74). For many silicates, only ions from the exposed surface layers are in a position to exchange. Typically grinding increases the exchange capacity of these minerals (41). For others, especially the zeolites, the lattice structure is open, permeated by waterfilled channels, and possess internally accessible exchange sites. Industrial applications of these and other synthetic aluminosilicates were limited by their low exchange capacity and instability under acid or alkaline conditions. The recent introduction of synthetic organic ion exchangers with superior properties

led to widespread industrial and laboratory exploitation of ion exchange and a resultant surge in research on ion exchange equilibria and kinetics. With these exchangers, it was possible for the first time to vary their properties systematically. Much of the theoretical advances made were due to this fact.

Ion exchange equilibria and kinetics are fundamental to an understanding of ion transport and have been studied intensively. As yet, no single comprehensive theory exists to explain all of the results involving ion exchange. Certain characteristics are normally common to all ion-exchange reactions. The reaction is usually reversible and always involves an equivalent exchange of ions. In addition, the exchanger preferentially adsorbs one ion over another, a property appropriately termed "selectivity."

Electrical double-layer theory (71) advanced by Helmholtz and modified by Gouy and Stern as an explanation of the electrokinetic properties of colloids has been utilized to explain the phenomena associated with ion exchange by soil clays (7,22,37). This theory adequately accounts for the preferential sorption of ions of higher valence over those of lower valence, but fails to explain observed exchanger selectivity among ions of equal valence. Bolt (8) attempted, with limited success, to extend the double layer theory to account for such behavior.

The overall ion exchange process can formally be represented as a reversible chemical reaction. The exchange of ions 1 and J of valence $\pm z_i$ and $\pm z_j$ respectively can be written as

$$z_j \, I|^{z_i}| + z_i \, \overline{J}|^{z_j}| \rightleftarrows z_j \, \overline{I}|^{z_i}| + z_i \, J|^{z_j}|$$

where the bar signifies the ion associated with the exchanger. As demonstrated by Kerr (42), the ion in combination with the exchanger could not be considered as a precipitate with unit activity. He assumed that the combination behaved as a solid solution, a view that was subsequently supported (5,11,72), and has gained wide acceptance by investigators studying ion exchange.

A useful quantity, the selectivity coefficient, characterizing the relative preference of the exchanger for the ions I and J was obtained by applying the law of mass action without activity corrections. Thus

$$K_J^I = \frac{\bar{C}_i^{|z_j|} \cdot C_j^{|z_i|}}{\bar{C}_j^{|z_i|} \cdot C_i^{|z_j|}} \qquad (21)$$

where C represents molar concentrations.

Except when $z_i = z_j$, the numerical value of K_J^I depends on the choice of concentration units. The total equivalent concentration $Co = z_i C_i + z_j C_j$ of ions I and J in the solution and the corresponding quantity $Qo = z_i \bar{C}_i + z_j \bar{C}_j$ associated with the exchanger must remain unchanged throughout the reaction. Defining $X_i = z_i C_i / C_o$ and $\bar{X}_i = z_i C_i / Q_o$ as the "equivalent ionic fractions" of the ion I in solution and exchanger respectively, and similar quantities for the ion J, yields

$$K_J^I = \frac{X_i^{|z_j|} \cdot \bar{X}_j^{|z_i|}}{\bar{X}_i^{|z_j|} \cdot X_j^{|z_i|}} \cdot \left(\frac{Co}{Qo}\right)^{|z_i| - |z_j|} \qquad (22)$$

The selectivity coefficient as defined is thus dependent on the total equivalent concentration of the exchanging ions in solution and the capacity of the exchanger. In addition, as shown by Bonner and Bonner

and Payne (9,10), it is also a function of the extent of exchange and assumes its highest value when the exchanger is completely saturated with ion J. The selectivity coefficient is thus not a particularly useful quantity for predicting ion exchange equilibria.

A thermodynamically rigorous application of the mass action law results in an expression for the thermodynamic equilibrium constant. This expression is

$$K^* = \frac{\bar{a}_i^{|z_j|} \cdot a_j^{|z_i|}}{a_i^{|z_j|} \cdot \bar{a}_j^{|z_i|}} \qquad (23)$$

where "a" represents ion activity. Determination of K* requires quantitative values for the activity coefficients of the exchanging ions in solution and in combination with the exchanger. This constitutes the difficulty in using the classical thermodynamic approach. The Debye-Huckel theory and its extensions to predict activities of electrolytes in solutions are applicable for concentration ranges below those normally associated with the solid solution concept. This difficulty is not insurmountable, however, because methods based on classical thermodynamics are available to determine the activity coefficients of ions in combination with the exchanger and the equilibrium constant (17,26). This treatment is of more theoretical than practical interest because it requires numerous measurements before the equilibrium constant can be determined (21,30).

Ion exchange as a Donnan system was introduced by Mattson and Larsson (47), and probably represents the most powerful concept in explaining ion exchange. It was mainly through the work of Bauman (5), Boyd (11) and Glueckauf (27) that this important concept has gained general acceptance. The quantitative principle involved in

the Donnan approach is essentially a generalization of the double layer concept, which is of universal occurrence whenever electrical charge is confined within a definite region of space. The Donnan approach imposes the thermodynamic condition that all other movable charges must adjust themselves accordingly to produce a minimum in the free energy of the system at equilibrium. The Donnan treatment thus represents a partial fusion of the electrostatic and thermodynamic aspects of the ion-exchange phenomenon.

Another approach likens the ion-exchange process to the physical adsorption of gases. Both the Langmuir and Freundlich equations have been used to describe data on ion exchange equilibria (11,37). There is a general concensus that ion exchange processes involve strong, long range electrostatic forces which were not considered in the conceptual development of the Langmuir and Freundlich equations. Only vague physical meanings can be attached to the parameters obtained from the application of these equations, and therefore, they have not provided much insight into the adsorption processes involved.

A novel and interesting simplified statistical approach has been used by Jenny (38) and Davis (18) to derive general theoretical equations for ion-exchange equilibrium. Although the results appear interesting, these concepts have not been used widely.

Although ion exchange can be represented formally as a chemical reaction, the physical processes involved have little in common with true chemical reactions. Evidence for this has appeared in equilibrium studies (42,72) where the ion in combination with the exchanger was treated as a solid solution. In addition, standard enthalpy changes

for ion-exchange reactions are often less than two kilocalories per mole which is typical of the orientation energies involved in dipole-dipole interactions. Such evidence indicates that ion exchange is essentially a statistical redistribution of the exchanging ions between the exchanger and the solution.

Further support for this concept was provided by the pioneering ion-exchange kinetic studies of Boyd, Adamson and Meyers (12). They obtained close agreement between their experimental data on exchange kinetics and predictions from theoretical equations based on the concept of ion exchange as a diffusion process. They hypothesized that either diffusion through a stagnant film around the particle or diffusion into the particle were rate controlling. Integrated rate equations for both cases were obtained by application of Ficks' laws for constant diffusion coefficients. The hypothetical stagnant film was assumed to have a finite thickness and was regarded as similar to the 'Nernst' film encountered in reactions at electrode surfaces. They found that either one or both mechanisms were rate-controlling and depended upon the experimental conditions. Their findings were immediately confirmed by other investigators (32,44,58). These studies showed that, in general, particle diffusion kinetics were favored for solution concentrations greater than 10^{-2} M, efficient mixing (which reduces film thickness), large particle size and low diffusion coefficients for ions in the exchanger. Opposite conditions were conducive to film-diffusion kinetics. Measurements of self-diffusion coefficients of cations in synthetic organic exchangers were made by Boyd and Soldano (13). In general, these were an order of magnitude

less than the corresponding values in solution and decreased with increasing valence.

A significant improvement in the analysis of the two step diffusion concept was introduced by Helfferich and his coworkers (34,36,56). They observed that Fick's first law did not take into account electrokinetic forces involved in the interdiffusion of two charged species. They introduced the more appropriate Nernst-Planck flux equation, which contained an additional electrical transference term. This equation is

$$J^* = -D\frac{\partial C}{\partial x} - \frac{zF}{RT} DC \frac{\partial \phi}{\partial x} \tag{24}$$

where J^* is flux of any charged species, F is the Faraday constant and ϕ is electrical potential. Equation (24) was derived for diffusion of charged particles in an electrical field assuming ideal systems and is widely used in the analysis of electrochemical reactions. The requirement that electroneutrality be maintained at all points in the system implies a rigid coupling of the concentrations and fluxes of the exchanging ions. Thus, for two ions I and J, electroneutrality requires

$$|z_i| C_i + |z_j| C_j = \text{constant} \tag{25a}$$

and

$$z_i J_i^* + z_j J_j^* = 0. \tag{25b}$$

These conditions allow the derivation of a single flux equation for either I or J. This equation is given (36) by

$$J_i^* = -\frac{D_i D_j (z_i^2 C_i + z_j^2 C_j)}{z_i^2 C_i D_i + z_j^2 C_j D_j} \frac{\partial C_i}{\partial x} \tag{26}$$

An immediate observation from this equation is that the interdiffusion flux is dependent on the relative concentrations of the inter-

diffusing ions. With vanishing concentration of either I or J the interdiffusion flux is controlled by the diffusion coefficient of the ion in the minority. Further analysis of the kinetic behavior of ion-exchange reactions by these investigators for both film and particle diffusion (36) led to the conclusion that the rates of forward and reverse exchange reactions were not equal. This conclusion was confirmed experimentally (34,35).

Incorporation of the simple diffusion-kinetics model based on Fick's law into the differential mass-transport equations produces a mathematical problem of extreme complexity (40). As a result simpler equations based on the linear diffusion concept introduced by Glueckauf (29) have been utilized (63). As pointed out by Helfferich in his comprehensive monograph on ion exchange (35), for practical situations, the gain in accuracy does not warrant the time and effort expended in solving the problem of greater complexity.

CHAPTER 2

SYNTHESIS OF PERTINENT THEORY ON INORGANIC ION EXCHANGE AND TRANSPORT PROCESSES

Thermodynamic Conceptualization of Ion-Exchange Processes

A system is defined thermodynamically as a body or group of interacting bodies intended for separate study. Any physically homogeneous body or set of identical homogeneous bodies is called a phase. Phases are either pure or mixed, depending on whether they consist of a single or several chemically individual species.

Systems are either homogeneous or heterogeneous depending on whether they consist of a single or several phases. The existence of physical boundaries (interfaces) and interphase regions are necessary features of polyphase systems. A solution/exchanger system can therefore be conceived thermodynamically as a heterogeneous system consisting of two mixed phases.

A heterogeneous system may exist either in an equilibrium or non-equilibrium state. In the former state all thermodynamic state variables remain constant with time. If the system is non-equilibrium, spontaneous phase interactions occur resulting in the establishment of an equilibrium state, characterized by definite compositions of all the phases. Interactions that do not involve the production of new phases or new chemical compounds result in material or energy exchanges across the interfaces. Such interactions are considered as physical sorption processes and involve atomic and molecular interaction

energies distinct from those involved in chemical bonds. The term adsorption refers to physical sorption in which the species transferred becomes either concentrated at the interface or distributed in the bulk of the phase. If instead of being transferred, the species is displaced by interactive forces back into the same phase it is termed negative adsorption or loosely as exclusion.

A unique property of exchanger phases in the presence of fixed electrical charge sites, which may be either restricted to the exchanger surface or distributed throughout its bulk volume. The quantity of fixed charges, conveniently expressed as equivalents, defines the absolute capacity of the exchanger. This property, coupled with the restriction that electroneutrality be satisfied at all points in either phase of the system, forms the basis for the metathetical sorption phenomena in solution/exchanger systems. Were it not for its fixed charges, the exchanger would lose its identity as a distinct phase in the system at equilibrium. Ion exchange processes occurring during equilibration of a solution/exchanger system can be considered as physical adsorption, if it is hypothesised that no interactions occur involving the formation of chemical bonds and production of new chemical species or phases in the system.

Disposition of Charged Species in Solution/Exchanger Systems at Equilibrium

For charged species in a heterogeneous system, a necessary condition at equilibrium is equality of the electrochemical potential of each species in the various phases. The electrochemical potential η for a species in a phase is defined (31) by

$$\eta = \mu + zF\phi \qquad (27)$$

in which μ is the chemical potential, z the valence, F the Faraday constant and ϕ the inner potential of the phase. The electrochemical potential can be conceived as the sum of the reversible chemical and electrical work required to transfer a charged particle from infinity to any point in the interior of the phase. If the particle is uncharged no electrical work is involved and $\eta = \mu$.

Consider two ions I, J of valence z_i, z_j in the solution/exchanger system at equilibrium. Then, $\eta_i = \bar{\eta}_i$ and $\eta_j = \bar{\eta}_j$, where the bar signifies the exchanger phase. The chemical potential for a species in a phase is given by

$$\mu = \mu^\circ + RT \ln a \tag{28}$$

where μ° is the chemical potential in an arbitrary reference state, R is the gas constant, T is absolute temperature and "a" is activity.

Substituting equation (28) into equation (27) and equating the electrochemical potentials of I and J gives

$$\bar{\mu}_i^\circ + RT \ln \bar{a}_i + z_i F \bar{\phi} = \mu_i^\circ + RT \ln a_i + z_i F \phi \tag{29a}$$

$$\bar{\mu}_j^\circ + RT \ln \bar{a}_j + z_j F \bar{\phi} = \mu_j^\circ + RT \ln a_j + z_j F \phi \tag{29b}$$

The difference in the inner potential of the phases $\bar{\phi} - \phi$, at equilibrium is invariable, and $\bar{\mu}_i^\circ = \mu_i^\circ$, $\bar{\mu}_j^\circ = \mu_j^\circ$. Thus

$$\bar{\phi} - \phi = \frac{RT}{z_i F} \ln \frac{a_i}{\bar{a}_i} = \frac{RT}{z_j F} \ln \frac{a_j}{\bar{a}_j} \tag{29c}$$

and

$$\frac{1}{z_i} \ln \frac{a_i}{\bar{a}_i} = \frac{1}{z_j} \ln \frac{a_j}{\bar{a}_j} \tag{29d}$$

Multiplying by $z_i z_j$ equation (29d) becomes

$$z_j \ln \frac{a_i}{\bar{a}_i} = z_i \ln \frac{a_j}{\bar{a}_j} \tag{29e}$$

whence

$$(\frac{a_i}{\bar{a}_i})^{z_j} = (\frac{a_j}{\bar{a}_j})^{z_i} \tag{29f}$$

Similar reasoning for an ion X of valence $-z_x$ yields

$$(\frac{\bar{a}_x}{a_x})^{z_i} = (\frac{a_i}{a_i})^{z_x} \quad \text{and} \quad (\frac{\bar{a}_x}{a_x})^{z_j} = (\frac{a_j}{\bar{a}_j})^{z_x} \tag{30}$$

Insight into the usefulness of the above relations can be obtained by considering some specific cases.

Consider an exchanger with fixed negative charges and absolute capacity Qo satisfied by J ions in equilibrium with a solution of an electrolyte $J_{z_x}X_{z_j}$. Electroneutrality requires

$$z_j\bar{C}_j = Q_o + z_x\bar{C}_x \quad \text{and} \quad z_jC_j = z_xC_x, \tag{31a}$$

where C represents the molar concentration. From above equation (29c) shows that

$$\bar{\phi} - \phi = \frac{RT}{z_jF} \ln \frac{a_j}{\bar{a}_j}$$

The potential difference $\bar{\phi} - \phi$ is the equilibrium Donnan potential across the interphase, and increases away from the solution/exchanger interface. The interphase functions as a Donnan membrane in a thermodynamic sense because it is impermeable to the fixed exchanger charges. This macroscopic potential is immediately established and is the force preventing the net transfer of J ions out of the exchanger and of X ions into the exchanger despite concentration differences that exist between the two phases. Increasing concentrations of J ions in solution causes a lowering of the Donnan potential while increasing the exchanger capacity would result in larger potentials. It is obvious that $\lim_{a_j \to \bar{a}_j} (\bar{\phi} - \phi) = 0$. If a dilute solution $J_{z_x}X_{z_j}$ is used for equilibration then $a_j \doteq C_j$ and $\bar{a}_j = \bar{\gamma}_j\bar{C}_j$, where γ denotes the activity coefficient. From equation (31a) it follows that

$$\bar{C}_j = \frac{Q_o + z_x \bar{C}_x}{z_j} \simeq \frac{Q_o}{z_j} \tag{31b}$$

From above equation (30) is

$$(\frac{\bar{a}_x}{a_x})^{z_j} = (\frac{a_j}{\bar{a}_j})^{z_x}$$

Substituting C_j for a_j and $\frac{\bar{\gamma}_j Q_o}{z_j}$ for $\bar{a}_j$ gives

$$(\frac{\bar{a}_x}{a_x})^{z_j} \simeq (\frac{C_j z_j}{\bar{\gamma} Q_o})^{z_x} \tag{31c}$$

Since $\bar{\gamma}_j Q_o$ is much larger than $C_j z_j$, the concentration of X in the exchanger is lower than in solution. This effect is greater the more dilute the solution of $J_{z_x}X_{z_j}$, and is enhanced with an increasing valence of the ion X. It is commonly called "Donnan exclusion."

If a salt $I_{z_x}X_{z_i}$ is now introduced into the system described above, exchange of I and J occurs. At equilibrium equation (29f) shows that

$$(\frac{a_j}{\bar{a}_i})^{z_j} = (\frac{a_j}{\bar{a}_j})^{z_i}$$

Rearranging gives

$$\frac{(\bar{a}_i)^{z_j}}{(\bar{a}_j)^{z_i}} = \frac{(a_i)^{z_j}}{(a_j)^{z_i}} \tag{32}$$

If I is introduced in a trace quantity, then $\bar{a}_j$ is approximately constant. With this condition, application of Le Chatelier's Principle to equation (32) shows that if the concentration of J is increased in the equilibrium solution then $\bar{a}_i$ decreases and vice-versa. Thus, for dilute solutions of $I_{z_x}X_{z_i}$ the presence of J ions in the solution phase will lower the selectivity of the exchanger for I ions. This effect will be greater the larger the difference between z_j and z_i.

From the general relation given by equation (29f)

$$(\frac{a_i}{\bar{a}_i})^{z_j} = (\frac{a_j}{\bar{a}_j})^{z_i}$$

Dividing throughout by $(\frac{a_j}{\bar{a}_j})^{z_i}$ results in

$$(\frac{a_i}{\bar{a}_i})^{z_j} \cdot (\frac{\bar{a}_j}{a_j})^{z_i} = 1. \qquad (33a)$$

Introducing activity coefficients gives

$$\frac{C_i^{z_j}}{\bar{C}_i^{z_j}} \cdot \frac{\bar{C}_j^{z_i}}{C_j^{z_i}} = \frac{\bar{\gamma}_i^{z_j}}{\gamma_i^{z_j}} \cdot \frac{\gamma_j^{z_i}}{\bar{\gamma}_j^{z_i}}. \qquad (33b)$$

The term on the left side of equation (33b) is the definition of the "selectivity coefficient" obtained by application of the mass action law without activity corrections for the exchange of I and J. Since the activity coefficients are functions of species concentration, the selectivity coefficient depends on the experimental conditions.

Physical Basis for Exchanger "Selectivity"

The power of thermodynamics is its ability to produce general relations among system variables without detailed knowledge of the specific physical forces involved in the phase interactions. These are concealed in the thermodynamic activities of the system components. The equilibrium composition of the phases is governed by the requirement that the free energy of the system be minimized. A charged species in a non-equilibrium solution/exchanger system can lower its free energy by interactions with the exchanger, solvent, and other ions in the system. Quantitative theories do not exist to predict exactly the effect of such interactions, generally termed solvation processes, on the thermodynamic properties of the phases. The sum total of all interactions reveals itself in the observed selectivity property of the exchanger. In effect, selectivity is a measure of the relative interactive effect of two exchanging ions on the thermodynamic properties of the exchanger phase.

In an aqueous solution/exchanger system, electroneutrality requires that the fixed charge on the exchanger be satisfied, at all times, by an equivalent quantity of charges of opposite sign. This fact determines the minimum equivalent concentration of the interstitial solution of porous exchangers. If Q_o represents the absolute capacity in equivalents per gram, ρ the dry bulk density, and f the fractional internal porosity of the exchanger particles, then $\rho Q_o/f$ equivalents/cm^3 is the concentration of the interstitial solution. An exchanger with Q_o = 100 meq/100g, ρ = 1 g/cm^3, and f = 0.5 gives a concentration of 2 N for the interstitial solution. Similar concentrations would occur in the interphase regions of exchangers with surface charge sites. In high capacity synthetic organic exchangers, values as high as 10 N are encountered. Such concentration ranges are beyond the scope of the Debye-Hückel theory for obtaining the thermodynamic effect of ion-ion interactions.

Ion-solvent effects can be evaluated by the Born theory. This theory gives the solvation free-energy per mole of ions in solution as

$$G = \frac{-N_A(ze)^2}{2(r + 0.85)} \left(1 - \frac{1}{\epsilon}\right) \tag{34a}$$

where N_A is Avogadro's number, z is the valence, r the crystal radius, e the electron charge, ϵ the dielectric constant, and 0.85 Å an empirical correction factor. The change in free energy in transferring one mole of I ions from solution to an exchanger in the J form due to ion-solvent interactions and electrical work would be

$$\vec{\Delta G} = \frac{-N_A(z_i e)^2}{2(r_i + 0.85)} \left(\frac{1}{\epsilon} - \frac{1}{\bar{\epsilon}}\right) + z_i F(\bar{\phi} - \phi) \tag{34b}$$

Since the exchanger solution is more concentrated $\bar{\varepsilon} < \varepsilon$ and the solvent interaction term is positive. Thus the transfer does not occur spontaneously unless the second term, which is negative, has a greater absolute value.

The transfer of I into the exchanger must be accompanied by an equivalent transfer of z_i/z_j moles of J out of the exchanger. For this process

$$\overleftarrow{\Delta G} = \frac{-z_j z_j N_A e^2}{2(r_j + 0.85)} \left(\frac{1}{\bar{\varepsilon}} - \frac{1}{\varepsilon}\right) + z_j F(\phi - \bar{\phi}) \qquad (34c)$$

In this case the leading term is negative and the electrical work term is positive. The total free energy change for the metathetical reaction is

$$\Delta G = \overrightarrow{\Delta G} + \overleftarrow{\Delta G}. \qquad (34d)$$

When $z_i = z_j$, ΔG is negative if $r_j < r_i$. Thus, considering only ion-solvent interactions, an exchanger with fixed charges neutralized by J has preference among ions of equal valence which would increase in order of increasing crystal radius. In part, ion-solvent interactions serve to explain selectivity among ions of equal valence. When $z_i \neq z_j$, the electrical work term dominates the solvation term and thus regardless of radius, the exchanger prefers the ion of higher valence.

The concept of exchanger selectivity as competitive solvation cannot be developed further because a complete understanding of these processes is far from being realized. However, the above does illustrate the complexity of the physical interactions involved in solution/exchanger systems.

Concepts on Inorganic Ion Transport During Miscible Displacement

Established concepts on ion-exchange equilibria and kinetics allow some qualitative deductions regarding the transport behavior of inorganic ions during miscible displacements.

If instantaneous exchange equilibrium is assumed, the transport behavior of an ion depends on the shape and characteristics of the adsorption isotherm. These would rest heavily upon the selectivity properties of the exchanger. Over a small range of very dilute concentrations of the equilibrating solution phase, it can be expected that the isotherms would be linear. In such ranges, for an exchanger saturated with J ions, the presence of J ions in the equilibrating solution would influence the sorption of another counterion in the system. As a result, variations in the concentration of J ions in a displacing solution of I ions would produce variations in the elution times for the ion I.

The two-step diffusion concept of exchange kinetics suggests that for small diameter exchanger particles and trace concentrations of I in the displacing solution, film-diffusion kinetics may control mass transfer of I. Since the film is considered as a stagnant hydrodynamic boundary layer around the exchanger particle, its thickness would be inversely influenced by flow velocity of the solution. Also, as discussed in the foregoing review [equation (26)], mass transfer of I by diffusion would be influenced by the presence of J ions. The existence of such rate-controlled diffusion processes would reflect in deviations from the predicted equilibrium shapes of elution curves for I.

CHAPTER 3

SOLUTION OF THE CONVECTIVE-DISPERSION EQUATION FOR A "PULSE INPUT" AND ITS EXTENSION FOR A SOLUTE FOLLOWING A LINEAR ISOTHERM

Although solutions to the convective-dispersion equation are often quoted and used, detailed derivations of these solutions are not usually presented. Details of an asymptotic solution to the convective-dispersion equation for "pulse input" boundary conditions are given below for a non-reactive and a reactive solute (linear adsorption isotherm).

The mathematical formulation of the problem is given by the equation

$$\frac{\partial C}{\partial t} = D\frac{\partial^2 C}{\partial x^2} - v\frac{\partial C}{\partial x} \quad \text{for } 0 < x < \infty \text{ and } t > 0 \tag{35}$$

with initial and boundary conditions

$$C(x,o) = 0, \quad \text{for } 0 < x < \infty \tag{36a}$$

$$C(0,t) = C_o[U(t) - U(t - t_1)], \quad \text{for } t > 0 \tag{36b}$$

$$\underset{x \to \infty}{C(x,t)} = 0, \quad \text{for } t > 0 \tag{36c}$$

where $U(t)$ is the Heaviside unit function and t_1 is the time-width of the pulse.

Let the Laplace transform of $C(x,t)$ be denoted by $u(x,s)$. The above equation and auxiliary conditions under the Laplace transformation become

$$su(x,s) - C(x,0) = D\frac{d^2u}{dx^2} - v\frac{du}{dx}. \tag{37}$$

$$u(0,s) = \frac{C_o}{s}(1 - e^{-st_1}). \tag{38a}$$

$$\lim_{x \to \infty} u(x,s) = 0. \tag{38b}$$

The characteristic equation of the ordinary differential equation is

$$Dm^2 - vm - s = 0. \tag{39a}$$

with roots $\frac{v \pm \sqrt{v^2 + 4Ds}}{2D}$.

Denoting $\frac{\sqrt{v^2 + 4Ds}}{2D}$ by R, the general solution is

$$u(x,s) = C_1 e^{(\frac{v}{2D} + R)x} + C_2 e^{(\frac{v}{2D} - R)x}. \tag{39b}$$

Applying the above initial and boundary conditions

$$u(0,s) = C_1 + C_2 = \frac{C_o}{s}(1 - e^{-st_1}). \tag{39c}$$

$$\lim_{x \to \infty} u(x,s) = 0 \Rightarrow C_1 = 0. \tag{39d}$$

Thus

$$u(x,s) = \frac{C_o}{s}(1 - e^{-st_1})e^{(\frac{v}{2D} - R)x}. \tag{39e}$$

$$= \frac{C_o}{s} e^{(\frac{v}{2D} - R)x} - \frac{C_o e^{-st_1}}{s} e^{(\frac{v}{2D} - R)x}. \tag{39f}$$

$$= C_o e^{\frac{vx}{2D}} \cdot \frac{e^{-Rx}}{s} - C_o e^{\frac{vx}{2D}} \cdot \frac{e^{-st_1} e^{-Rx}}{s} \tag{39g}$$

Consulting a table of Laplace transforms (60), transform pair #3.2-80 is listed as

$$\frac{1}{s} e^{-a(s + b^2)^{1/2}} \longleftrightarrow \frac{e^{-ab}}{2} \operatorname{erfc}\left(\frac{a}{2t^{1/2}} - bt^{1/2}\right) + \frac{e^{ab}}{2} \operatorname{erfc}\left(\frac{a}{2t^{1/2}} + bt^{1/2}\right)$$

valid for real $s > 0$.

Since

$$e^{-Rx} = e^{-\left(\frac{\sqrt{v^2 + 4Ds}}{2D}\right)x} = e^{-\frac{x}{2D}\sqrt{4D\left(\frac{v^2}{4D} + s\right)}}$$

$$= e^{-\frac{x}{\sqrt{D}}\sqrt{\frac{v^2}{4D} + s}} \qquad (40)$$

letting $a = \frac{x}{\sqrt{D}}$ and $b = \frac{v}{2\sqrt{D}}$, the first term inverts to

$$\frac{C_o}{2} e^{\frac{vx}{2D}} \{e^{-\frac{vx}{2D}} \operatorname{erfc}\left(\frac{x}{2\sqrt{Dt}} - \frac{vt^{1/2}}{2\sqrt{D}}\right) + e^{\frac{vx}{2D}} \operatorname{erfc}\left(\frac{x}{2\sqrt{Dt}} + \frac{vt^{1/2}}{2\sqrt{D}}\right)\} \qquad (41a)$$

$$= \frac{C_o}{2} \{\operatorname{erfc}\left(\frac{x - vt}{2\sqrt{Dt}}\right) + e^{\frac{vx}{D}} \operatorname{erfc}\left(\frac{x + vt}{2\sqrt{Dt}}\right)\} \qquad (41b)$$

The second term is inverted by noting that it is equal to the first term $x\, e^{-st}$. By the shifting property of the Laplace transforms, if $L\{f(t)\} = f(s)$, and $g(t) = f(t - t_1)$. $U(t - t_1)$ then, $L\{g(t)\} = e^{-st_1} f(s)$. The second term inverts to

$$\frac{C_o}{2} \{\operatorname{erfc}\left[\frac{x - v(t - t1)}{2\sqrt{D(t - t_1)}}\right] + e^{\frac{vx}{D}} \operatorname{erfc}\left[\frac{x + v\ (t - t1)}{2\sqrt{D(t - t_1)}}\right]\} \cdot U(t - t_1) \qquad (42)$$

The second term in both inverse transforms is small except near the inlet where $x = 0$ and for small values of t unless D is large. As a result it can be ignored without introducing a serious error. The solution reduces to

$$\frac{C}{C_o} = 1/2\{\operatorname{erfc}\left(\frac{x - vt}{2\sqrt{Dt}}\right) - \operatorname{erfc}\left[\frac{x - v(t - t1)}{2\sqrt{D(t - t_1)}}\right] U(t - t_1)\} \qquad (43a)$$

Using the identity $\operatorname{erfc}(x) = 1 - \operatorname{erf}(x)$, this can be written as

$$\frac{C}{C_o} = 1/2\{\operatorname{erf}\left[\frac{x - v(t - t_1)}{2\sqrt{D(t - t_1)}}\right] \cdot U(t - t_1) - \operatorname{erf}\left(\frac{x - vt}{2\sqrt{Dt}}\right)\} \qquad (43b)$$

It is convenient to use a transformed variable $\theta = \frac{vt}{L}$, which is physically equivalent to the number of pore volumes, for experiments with a fixed value of $x = L$. Setting $x = L$ and dividing the arguments

of the error functions in equation (43b) top and bottom by L, the solution given by equation (43b) transforms into

$$\frac{C}{C_o} = 1/2\{\text{erf}[\frac{1 - \theta + \theta_1}{2\sqrt{\frac{D(\theta - \theta_1)}{vL}}}] \cdot U(\theta - \theta_1) - \text{erf}(\frac{1 - \theta}{2\sqrt{\frac{D\theta}{vL}}})\} \quad (43c)$$

For a solute following a linear isotherm, $S = KC$, and $\frac{\partial S}{\partial t} = K\frac{\partial C}{\partial t}$. The differential equation becomes

$$\frac{\partial C}{\partial t} = D\frac{\partial^2 C}{\partial x^2} - v\frac{\partial C}{\partial x} - \frac{\rho K}{\theta_v}\frac{\partial C}{\partial t} . \quad (44a)$$

Transposing $\frac{\partial C}{\partial t}$ and rearranging

$$\frac{\partial C}{\partial t} = \frac{D}{R}\frac{\partial^2 C}{\partial x^2} - \frac{v}{R}\frac{\partial C}{\partial x} \quad (44b)$$

where $R = 1 + \frac{\rho K}{\theta_v}$.

For the same initial and boundary conditions it is obvious that the solution to equation (44b) can be obtained by setting $D = D/R$ and $v = v/R$ in the solution given by equation (43b). This yields after introduction of $\theta = \frac{vt}{L}$ and rearrangement

$$\frac{C}{C_o} = 1/2\{\text{erf}[\frac{(R - \theta + \theta_1)\sqrt{vL}}{2\sqrt{D(\theta - \theta_1)R}}] U(\theta - \theta_1) - \text{erf}[\frac{(R - \theta)\cdot\sqrt{vL}}{2\sqrt{D\theta R}}]\} \quad (45)$$

Equation (45) reduces to equation (43c) when $R = 1$. The former equation can therefore be used to generate theoretical elution curves for both reactive and non-reactive solutes, with given values of the parameters v, L, D, R and θ_1. Equation (45) was obtained assuming a semi-infinite space domain but it can be used to analyse displacement experiments in finite columns. It has been shown (14, 46, 54) that for large values of v and L no serious error is involved in using equation (45) for this purpose.

CHAPTER 4

EXPERIMENTAL OBJECTIVES, MATERIALS AND METHODS

The primary objective of this study was to examine the transport behavior of selected inorganic cations during steady saturated or unsaturated flow in a reactive porous medium. It was anticipated that these results would provide insight into the nature of the metathetical mass transfer processes.

From the onset, it was clear that soils were too heterogeneous to study exchange processes in detail. Therefore, a mixture was prepared with a synthetic exchange material and sand. Synthetic exchangers were utilized previously in miscible displacement studies by Day and Forsythe (20). In addition to providing the required homogeneity, the overall exchange capacity could be controlled.

A rigid, analytical grade, macroporous, granular (50 - 100 mesh), organic exchange resin of a highly crosslinked sulphonated copolymer of styrene with divinylbenzene was purchased (Bio-Rad Laboratories). This material is both thermally and chemically stable and has a cation exchange capacity of 4.9 meq/g. In addition, special treatment during polymerisation results in a low resistance to intra-particle mass transfer by diffusion. Preparation of synthetic organic exchangers in general has been described by Helfferich (35). Their general physical properties have been reviewed by Meyers et al. (48) and the special physical and chemical properties of the macroporous resins have been described by Miller et al. (49,50). Because of its high exchange capacity, it

was necessary to dilute this resin with an inert material. Soil from the 1 m - 1.3 m horizon of a Lakeland sand (Typic Quartzipsamment) was passed through a nest of sieves and the fractions retained on the 500, 250 and 105-micron sieves were combined in the ratio of 25 : 50 : 25, respectively. This material was then treated with hydrogen peroxide to destroy any organic matter present. The resin was treated repeatedly with 1 N calcium acetate solution until no further pH change was observed, and then packed into a plastic column and eluted with 1 N $Ca(NO_3)_2$ solution. This procedure was considered sufficient to Ca-saturate the resin. The resin was then dried and sieved and the fraction between 200 and 105 microns combined with the sand to yield a computed exchange capacity of 30 - 40 meq/100 g. This porous exchange material was used in all subsequent studies.

Cations selected for investigation were Li^+ and Na^+ because of their ease of detection at low concentrations by flame spectrophotometry. Calcium was chosen as the common ion because the Ca-saturated exchanger was expected to exhibit low selectivity for Li^+ and Na^+ resulting in low residence times. Because of this, longer columns could be used. The exclusion of Cl^- by the exchanger was also studied and a cursory investigation was made of the transport behavior of $^{45}Ca^{2+}$.

The columns to contain the exchange medium were prepared from a single length of rubber-cast plexiglass tubing with an internal diameter of 5.0 cm. The columns were designed to provide unsaturated flow conditions. To achieve unsaturation, 3-mm holes were drilled in the walls of the column, and small pieces of wire gauze (less than

100-micron mesh) were placed on the inside to retain the material in the column. Porous end-plates with an air-entry pressure of 30 - 40 cm of water were used to retain the material tightly in the columns. The dead volume of the end plates did not exceed 7 cm^3. The holes in the column were plugged during saturated flow studies. For unsaturated flow studies the holes were not plugged and the column was sealed into a 10-cm diameter column. The outer column was pressurized to achieve the desired unsaturated soil-water potential and the pressure was kept constant with a bubble tower.

The solid matrix material was packed into the column under water to insure complete water saturation. An adjustable peristaltic pump was used to deliver solution at predetermined rates to the columns. A fraction collector was used to sample the effluent at equal time intervals. A schematic of the experimental apparatus is given in Figure 1.

Molar stock solutions of $Ca(NO_3)_2$, NaCl, LiCl, $LiNO_3$ and $NaNO_3$ were prepared. Tracer solutions were prepared by combining suitable portions of the required stock solutions and making up to volume. The concentration of Na^+, Li^+ and Cl^- in the tracer solutions were kept between 80 - 85 ppm. Concentrations of the common ion (Ca^{2+}) used were 0.05 M, 0.02 M and 0.005 M. Tritiated water (HTO) was added as a non-reactive tracer to evaluate hydrodynamic dispersion. The transport of $^{45}Ca^{2+}$ was studied using tracer solutions prepared by dissolving one gram of $^{45}CaSO_4$ in 2 liters of 0.075 M and 0.05 M $Ca(NO_3)_2$.

Exchange isotherms for Na^+ and Li^+ in 0.05 M, 0.02 M and 0.005 M $Ca(NO_3)_2$ were determined over a 0 - 200 ppm concentration range. Ten

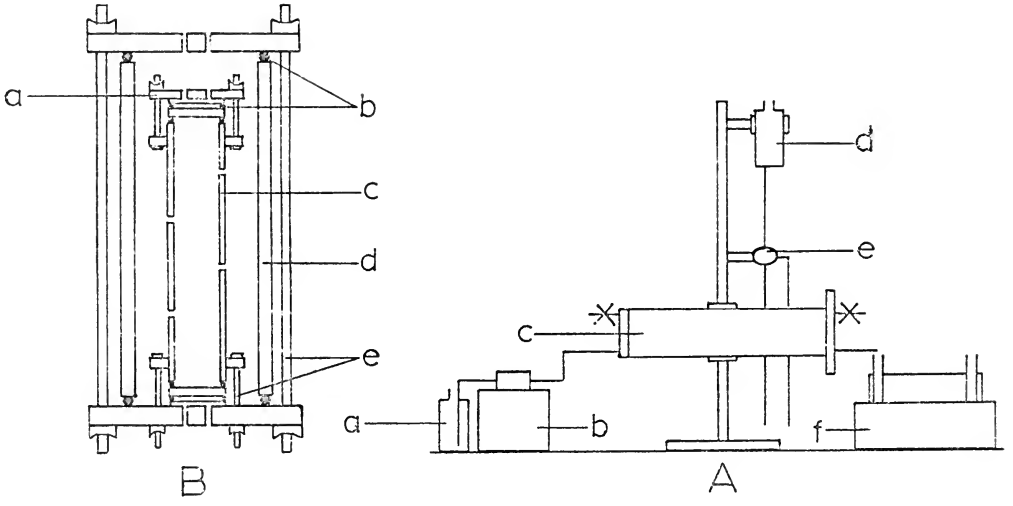

Figure 1. (A) Schematic of the flow system where a is a bottle with solution, b a peristaltic pump, c the column, d a flushing bottle, e a 3-way stopcock and f a fraction collector.
(B) Detail of column in outer chamber showing a end plate, b O-rings, c column, d outer chamber and e threaded bolts.

solutions in increments of 20 ppm were prepared by weighing out the required amounts of 2000 ppm stock solutions and making it up to volume with the appropriate $Ca(NO_3)_2$ solution. Ten-gram portions of the dry solid matrix material, previously washed with deionized water, were mixed with 10-ml portions of each solution and shaken at frequent intervals during a 12-hour period. This time was shown to be sufficient for equilibration. A sample of the supernatant was then withdrawn and analyzed. The amount adsorbed was calculated from the concentration difference between the sample and original solution. A similar technique was used to determine exchange isotherms for $^{45}Ca^{2+}$ in 0.075 M and 0.05 M $Ca(NO_3)_2$.

The 'pulse input' boundary condition was utilized in all miscible displacement studies. The columns were leached with appropriate tracer-free solutions of $Ca(NO_3)_2$ and then a pulse of the tracer solution containing the cation plus chloride and HTO was introduced. This pulse was subsequently eluted with the tracer-free $Ca(NO_3)_2$ solution. Changeover of solutions was achieved in approximately 2 minutes during which time the outlet was sealed, and the front end-plate and delivery tubing were flushed and refilled with the new solution. The total amount of solution introduced during a displacement was determined by weight differences in the bottles containing the solutions. These together with the measured time, were used in computing an average pore-water velocity.

Analysis for Li^+ and Na^+ in the effluent samples were made using a Beckman model B flame spectrophotometer. Sets of standard solutions for these analyses were prepared by accurate dilution of a 2000 ppm

stock with the appropriate $Ca(NO_3)_2$ solutions. Analyses for Cl^- were made using an "Orion" specific-ion electrode. Activity of HTO and $^{45}Ca^{2+}$ was determined by liquid scintillation counting of 1-ml samples, in 10 ml of a commercial phosphor (Aquasol II).

The pore volume of the columns was determined by drying the material in the column at the end of a series of displacements. The dispersion coefficients were extracted from the breakthrough data for HTO using a least squares curve-fitting procedure and the simplified asymptotic solution [equation (43c)]. These coefficients were then used to generate analytical curves for the reactive solutes using the sorption parameters from the adsorption isotherms.

CHAPTER 5

RESULTS AND DISCUSSION OF STUDIES ON EXCHANGE EQUILIBRIA AND TRANSPORT OF Na^+, Li^+, $^{45}Ca^{2+}$ AND Cl^-

Exchange Adsorption Isotherms

The adsorption isotherms for Na^+ and Li^+ in 0.05 M, 0.02 M and 0.005 M $Ca(NO_3)_2$ on the exchange mixture are given in Figures 2 and 3. The adsorption isotherms were linear for both Na^+ and Li^+ over the 0 to 200 ppm concentration range. The slope of the adsorption isotherm increased as the Ca^{2+} concentration in the equilibrating solution decreased.

The data in Figures 2 and 3 were fitted by the least squares procedure to the equation for a linear isotherm, $S = K C$. The resulting K values for Na^+ in 0.05 M, 0.02 M and 0.05 M $Ca(NO_3)_2$ were 0.1324, 0.2196 and 0.3770, respectively. The corresponding values for Li^+ were 0.0822, 0.1122 and 0.1534. These K values increase in a non-linear fashion with decreasing Ca^{2+} concentration in the equilibrating solution. As shown in Figure 4, an assumed general exponential relationship of the form $K = K_o \exp [\beta C_{Ca}]$ fitted the data reasonably well. For Na^+, the values of K_o and β were 0.3883 and -9.7 and for Li^+ the corresponding values were 0.1568 and -5.80. These values provide useful quantitative insight into the damping effect of the Ca^{2+} on the adsorption of Na^+ and Li^+.

From the theoretical considerations discussed previously [equation (32)] for equilibrium conditions the following relationship holds:

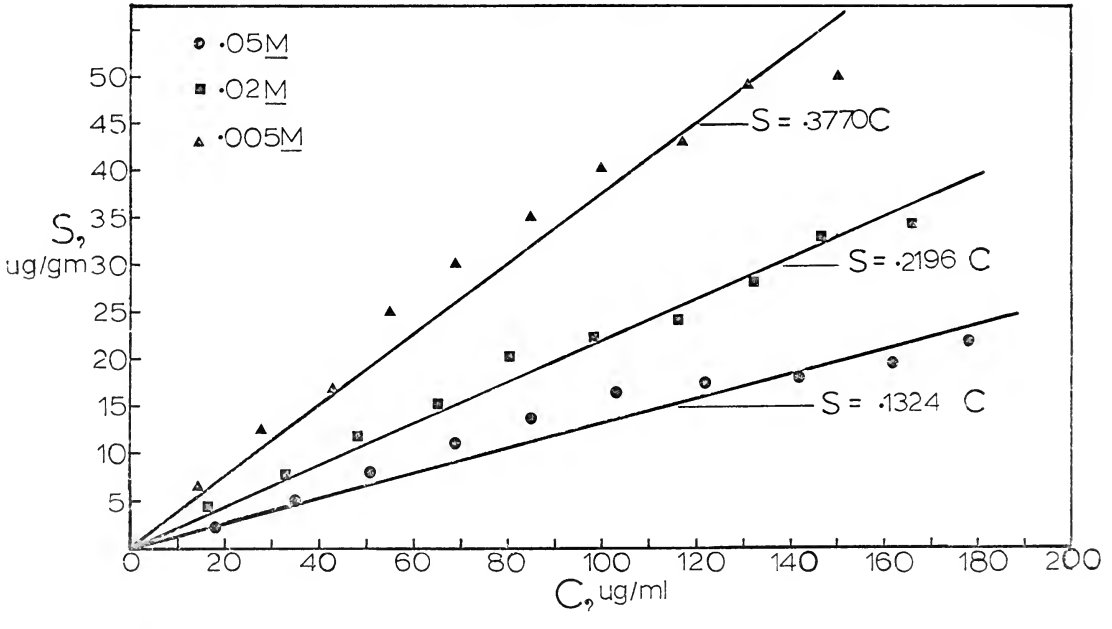

Figure 2. Exchange adsorption isotherms for Na^+ in 0.05 M, 0.02 M, and 0.005 M $Ca(NO_3)_2$. Solid lines are least squares fits to the equation S = KC.

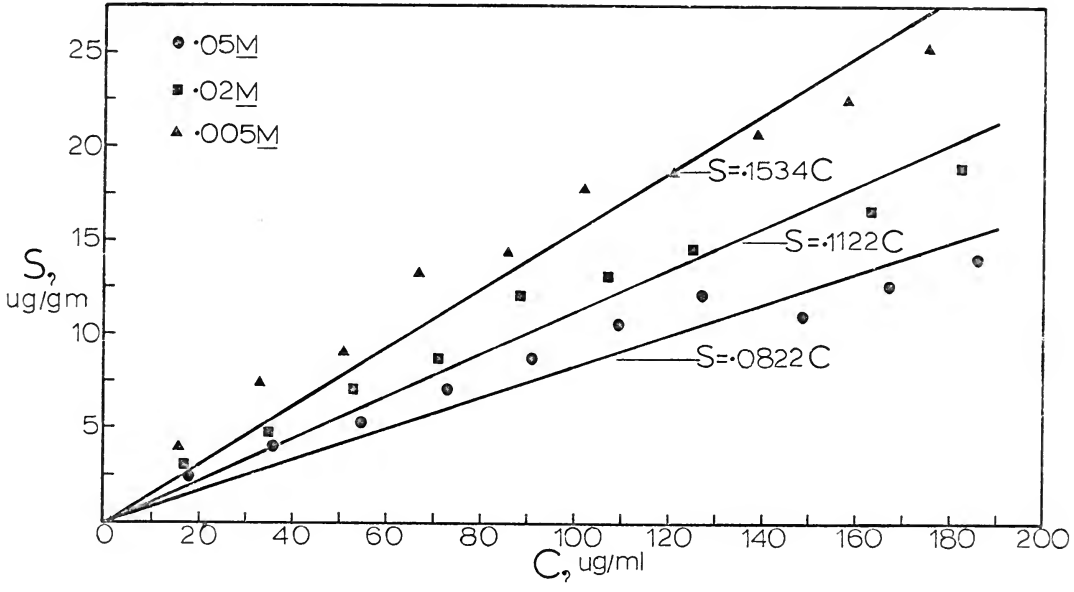

Figure 3. Exchange adsorption isotherms for Li^+ in 0.05 M, 0.02 M, and 0.005 M $Ca(NO_3)_2$. Solid lines are least squares fits to the equation S = KC.

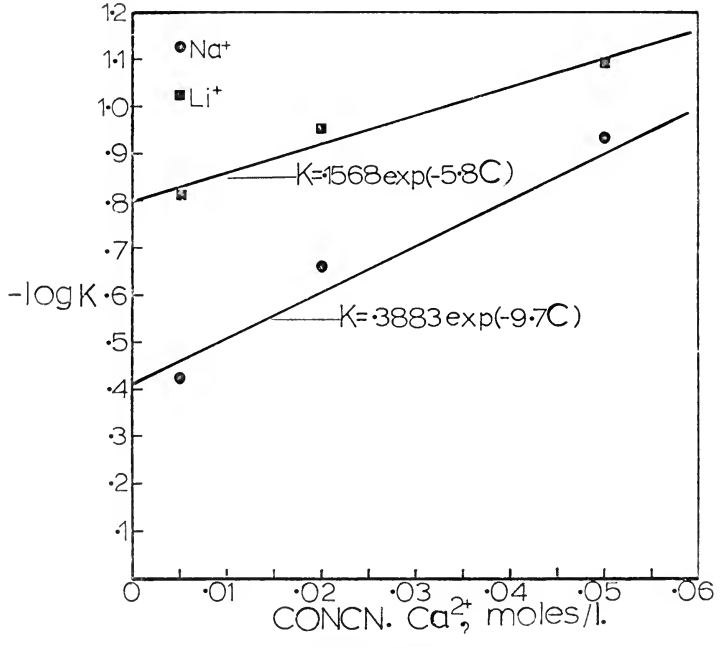

Figure 4. Dependence of the isotherm K values for Na^+ and Li^+ on the concentration (C) of Ca^{2+} in the equilibrium solution. Solid lines are least squares fits to the linearised equation $K = K_o \exp(\beta C_{Ca})$.

$$\frac{a^{2}_{Na}}{a_{Ca}} = \frac{\bar{a}^{2}_{Na}}{\bar{a}_{Ca}} \tag{46}$$

For the concentrations used in this study, both a_{Na} and a_{Ca} are accessible from the extended Debye-Hückel theory. This theory allows calculation of the activity coefficient from the following relationship:

$$-\log \gamma = \frac{Az^{2}\sqrt{I}}{1 + Ba\sqrt{I}} \tag{47}$$

where γ is the activity coefficient, $I = \frac{1}{2}\sum C_i z_i^2$ and is the ionic strength of the solution, A = 0.507 at 20 C, B = 0.328 at 20 C and α is the ion-size parameter. The value of α is 6 for Li^+ and Ca^{2+} and 4 for Na^+ (43). If only small quantities of Na^+ are adsorbed in the exchanger phase one can assume that $\bar{a}_{Ca}$ is constant. If it is further assumed that $\bar{\gamma}_{Na}$ remains constant, then $\bar{C}_{Na} = \frac{\rho S_{Na}}{f}$ may be substituted into equation (46) to give

$$\frac{a_{Na}}{\sqrt{a_{Ca}}} = \frac{\rho\bar{\gamma}_{Na}}{f\sqrt{\bar{a}_{Ca}}} \quad S_{Na} = K_1 S_{Na} \tag{48a}$$

Rearranging

$$\frac{\gamma_{Na}\, C_{Na}}{\sqrt{\gamma_{Ca} C_{Ca}}} = K_1 S_{Na} \tag{48b}$$

or

$$S_{Na} = \frac{\gamma_{Na}}{K_1\sqrt{\gamma_{Ca} C_{Ca}}}\, C_{Na} \tag{48c}$$

If K_1 is known, the K value for each adsorption isotherm can be computed.

It is recognized that since I varies with the Na^+ concentration in the equilibrating solution, both γ_{Na} and a_{Ca} are not true constants; however, their range of variation can be determined. For the experimental isotherm with Na^+ in 0.05 M $Ca(NO_3)_2$ over the 0 - 200 ppm Na^+ range, a minimum calculated value of 0.15 M for I is obtained using the above

formula. From the measured data for this isotherm a maximum value of I can be obtained. When the highest concentration of 200 μg/ml was used, the measured equilibrium values were S = 22 μg/g and C_{Na} = 178 μg/ml. Assuming that anions are excluded completely by the exchanger, the concentration of ionic species in the solution phase was Na^+ = 0.0077 M, Ca^{2+} = 0.0505 M, Cl- = 0.0057 M and NO_3^- = 0.10 M giving I = 0.161 M. The computed values for γ_{Na} for I = 0.15 M and I = 0.161 M are 0.740 and 0.735, respectively. Corresponding values for $\sqrt{a}_{Ca}$ are 0.134 and 0.132. Thus, the values of γ_{Na} and $\sqrt{a}_{Ca}$ do not vary appreciably between the maximum and minimum I values. However, it is clear that with decreasing concentration of $Ca(NO_3)_2$ in the equilibrating solutions, the gap between the maximum and minimum values of γ_{Na} and $\sqrt{a}_{Ca}$ does increase. As a realistic approximation, an average value of I = 0.155 M can be used to compute values of γ_{Na} and $\sqrt{a}_{Ca}$ with the extended Debye-Hückel formula. These calculations yield γ_{Na} = 0.7381 and $\sqrt{a}_{Ca}$ = 0.1331. Utilizing these values and the experimental K value of 0.1324 for this isotherm, a value of $K_1 = \gamma_{Na}/K\sqrt{a}_{Ca}$ can be calculated. If the above reasoning and assumptions are correct, this value of K_1 may be used to predict the experimental K values for the adsorption isotherms using 0.02 M and 0.005 M $Ca(NO_3)_2$. Similar arguments can be advanced for the equilibrium isotherms of Li^+.

With the above approach, K values for the isotherms of Na^+ in 0.02 M and 0.005 M $Ca(NO_3)_2$ were predicted using a calculated K_1 value of 41.9 and mean I values of 0.064 M and 0.020 M. These predicted K values were 0.201 and 0.347 which compares favorably with the measured values of 0.2196 and 0.3770, respectively. Similar computations for Li^+ using K_1 = 70.18 and mean I values of 0.079 M and 0.025 M,

yielded predicted K values for the Li^+ adsorption isotherms in 0.02 M and 0.05 M $Ca(NO_3)_2$ of 0.121 and 0.199 which compared reasonably well with the measured values of 0.112 and 0.153.

Implicit in the use of the Debye-Hückel theory is the assumption that the activities of the ions in the exchanger and solution phases are predominantly the result of electrostatic ion-ion interactions. The foregoing theoretical results confirm the validity of this assumption and underscores the importance of such interactions in ion-exchange equilibria.

The exchange adsorption isotherms for $^{45}Ca^{2+}$ in 0.075 M and 0.05 M $Ca(NO_3)_2$ are given in Figure 5. These were linear over the $^{45}Ca^{2+}$ concentrations used and illustrate a similar decrease in the K value with an increase in $^{40}Ca^{2+}$ concentration in the equilibrating solution.

Assuming that $^{45}Ca^{2+}$ and $^{40}Ca^{2+}$ are indistinguishable, then $\bar{\gamma}^{45}_{Ca} = \bar{\gamma}^{40}_{Ca}$ and $\gamma^{45}_{Ca} = \gamma^{40}_{Ca}$. This implies that there are no differences in their physical interactions to produce selectivity. With the previous theoretical considerations [equation (33b)], and using a dagger to distinguish between properties of $^{45}Ca^{2+}$ and $^{40}Ca^{2+}$

$$\frac{C^\dagger \cdot \bar{C}}{\bar{C}^\dagger \cdot C} = \frac{\bar{\gamma}^\dagger \cdot \gamma}{\gamma^\dagger \cdot \bar{\gamma}} = 1 \tag{49a}$$

whence

$$\frac{C^\dagger}{C} = \frac{\bar{C}^\dagger}{\bar{C}} \tag{49b}$$

At low concentrations of $^{45}Ca^{2+}$ both $\bar{C}$ and C can be regarded as constant.

Then

$$\bar{C}^\dagger = \frac{\bar{C}}{C} \cdot C^\dagger \tag{49c}$$

and

$$S^\dagger = \frac{K_1}{C} C^\dagger \tag{49d}$$

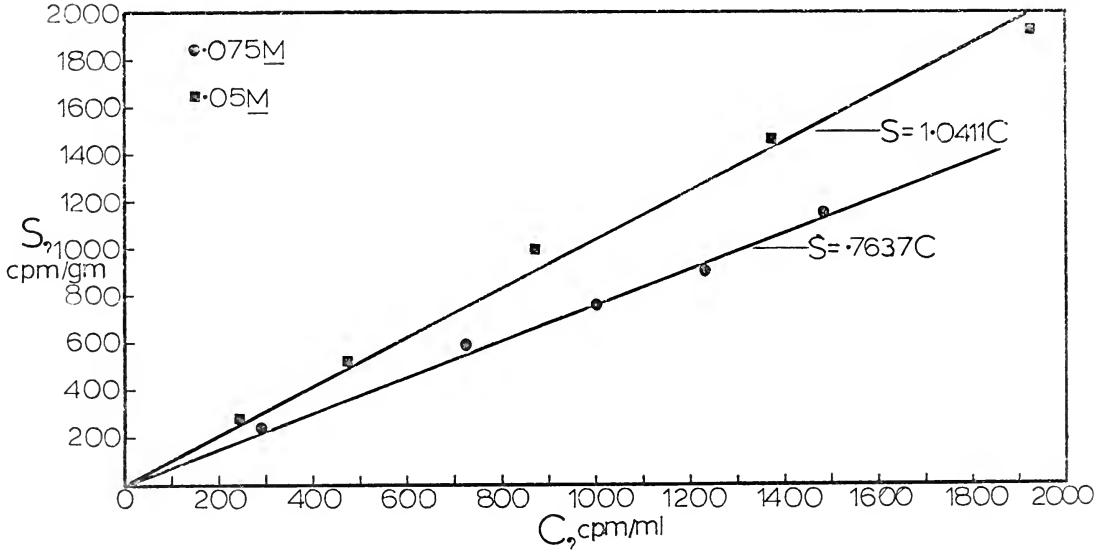

Figure 5. Exchange adsorption isotherms for $^{45}Ca^{2+}$ in 0.075 M and 0.05 M $Ca(NO_3)_2$. Solid lines are least squares fits to the equation S = KC.

in which K_1 embraces $\bar{C}$ and all factors involved in adjustment of units. Employing the same approach as that used for Na^+ and Li^+, it is possible to compute K_1 using the experimental K value of one adsorption isotherm. This value can then be used to predict the K value of other isotherms. This approach provides an evaluation of the validity of equation (49d). The experimental K value of the isotherm for $^{45}Ca^{2+}$ in 0.075 $\underline{M}$ $Ca(NO_3)_2$ is 0.764 which gives $K_1 = 0.057$. The predicted K value of the isotherm for $^{45}Ca^{2+}$ in 0.05 $\underline{M}$ $Ca(NO_3)_2$ was 1.146 which compares favorably with the measured value of 1.041.

The exchange adsorption isotherms for $^{45}Ca^{2+}$ are of interest in explaining the basis for the effect of increasing $^{40}Ca^{2+}$ concentrations on the K values. Consider specifically the exchanger in equilibrium with 0.05 $\underline{M}$ $Ca(NO_3)_2$ solution. If a Donnan electrostatic potential difference is set up across the interphase region, this essentially equalizes the diffusion rates of Ca^{2+} ions into and out of the exchanger allowing the continued existence of a higher concentration of Ca^{2+} in the exchanger phase to maintain electroneutrality. Although macroscopically the composition of either phase remains fixed, microscopic exchange of Ca^{2+} ions continues to occur at a fixed rate across the phase boundary. If some fixed amount of $^{45}Ca^{2+}$ ions is introduced in the solution, it is reasonable to expect that at equilibrium the $^{45}Ca^{2+}$ ions entering the exchanger depend solely on their relative abundance to $^{40}Ca^{2+}$ in the solution. Increasing the solution concentration of $^{40}Ca^{2+}$ to 0.075 $\underline{M}$ would reduce the relative concentration of $^{45}Ca^{2+}$ to $^{40}Ca^{2+}$ on the exchanger and thus the macroscopic adsorption of $^{45}Ca^{2+}$ is decreased. It is therefore reasonable to assume that the ratio of $^{45}Ca^{2+}$ in the exchanger and $^{45}Ca^{2+}$ in the solution is inversely propor-

tional to the concentration of $^{40}Ca^{2+}$ in the solution. Expressed quantitatively, $K_{.05}/K_{.075} = 0.075/0.05$ which is what was concluded above [equation (49d)] using a different approach. The foregoing results serve to give credence to the concept of ion exchange as a Donnan-type redistribution of ions between the solution and exchanger phases.

It was not possible to determine the negative adsorption isotherms for Cl^- in batch studies because the increases in Cl^- concentration were too small to detect above random variations associated with the specific-ion electrode.

Miscible Displacement Experiments with Na^+

Elution curves are presented in Figures 6 through 14 for a series of input pulses containing Cl^-, HTO and Na^+ in 0.05 M, 0.02 M or 0.005 M $Ca(NO_3)_2$, using three pore-water velocities ranging from 1.5 to 15 cm/hr for each $Ca(NO_3)_2$ concentration. These displacements were made using a 30.4-cm long column. The medium was packed to a bulk density (ρ) of 1.786 g/cm^3 and had a saturated, fractional volumetric water content, θ_v, of 0.344. Areas under the breakthrough curves in Figures 6 through 14 were determined by trapezoid rule integration and in each case indicated complete recovery of the material injected. Thus, complete reversibility of the mass transfer processes was achieved in these column studies.

It was not possible to maintain identical values of the three pore-water velocities for each concentration of $Ca(NO_3)_2$. However, in no case did the measured pore-water velocity deviate by more than $\pm$ 2% of the mean values (14.69, 7.29 and 1.52 cm/hr) taken over the three $Ca(NO_3)_2$ concentrations. Dispersion coefficients were determined from

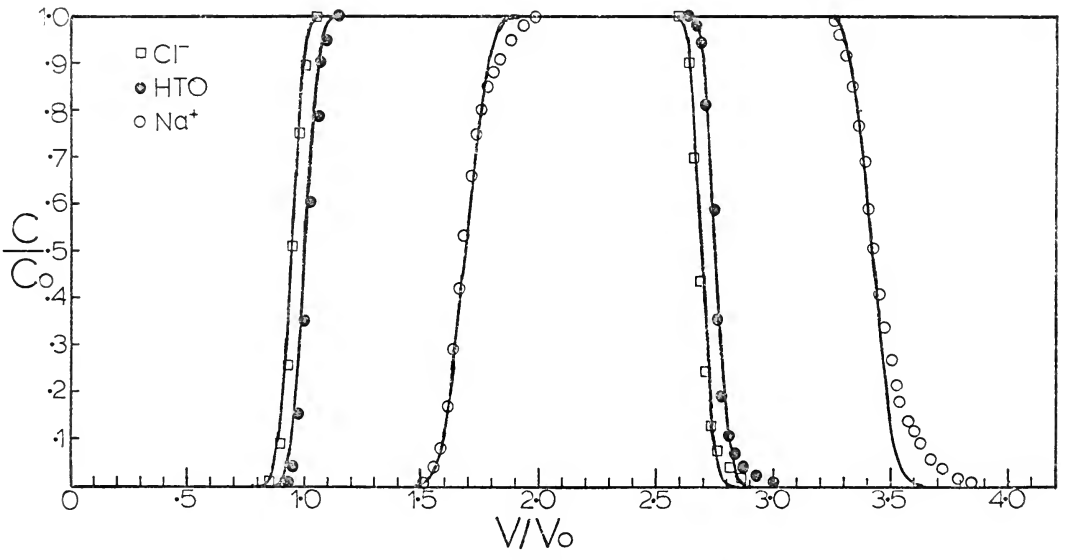

Figure 6. Elution curves for a "pulse input" of Na^+, Cl^-, and HTO in 0.05 M $Ca(NO_3)_2$ at a pore-water velocity between 14 and 15 cm/hr. Solid lines were calculated using equation (45).

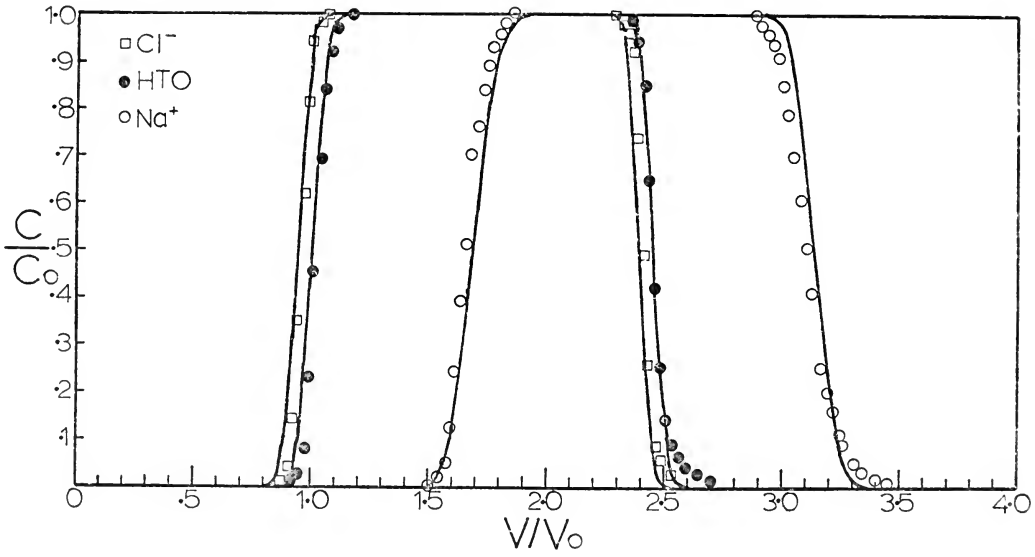

Figure 7. Elution curves for a "pulse input" of Na^+, Cl^-, and HTO in 0.05 M $Ca(NO_3)_2$ at a pore-water velocity between 7 and 8 cm/hr. Solid lines were calculated using equation (45).

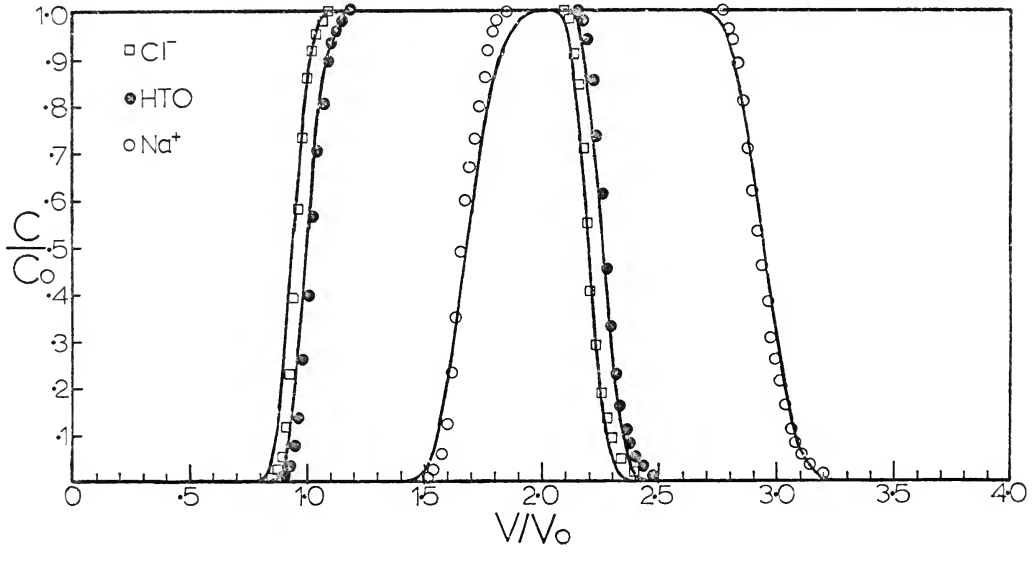

Figure 8. Elution curves for a "pulse input" of Na^+, Cl^-, and HTO in 0.05 M $Ca(NO_3)_2$ at a pore-water velocity between 1 and 2 cm/hr. Solid lines were calculated using equation (45).

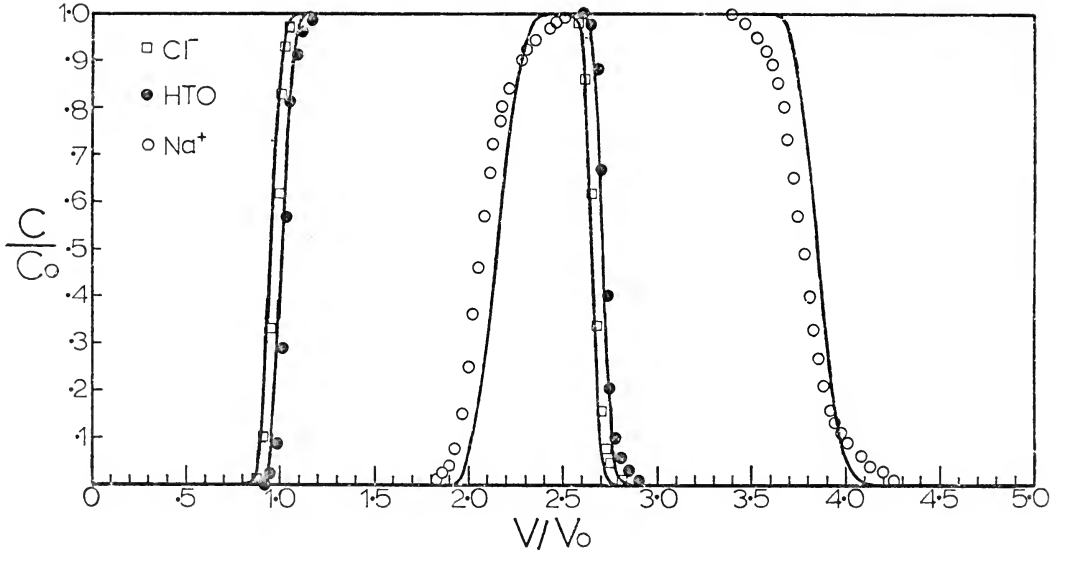

Figure 9. Elution curves for a "pulse input" of Na^+, Cl^-, and HTO in 0.02 M $Ca(NO_3)_2$ at a pore-water velocity between 14 and 15 cm/hr. Solid lines were calculated using equation (45).

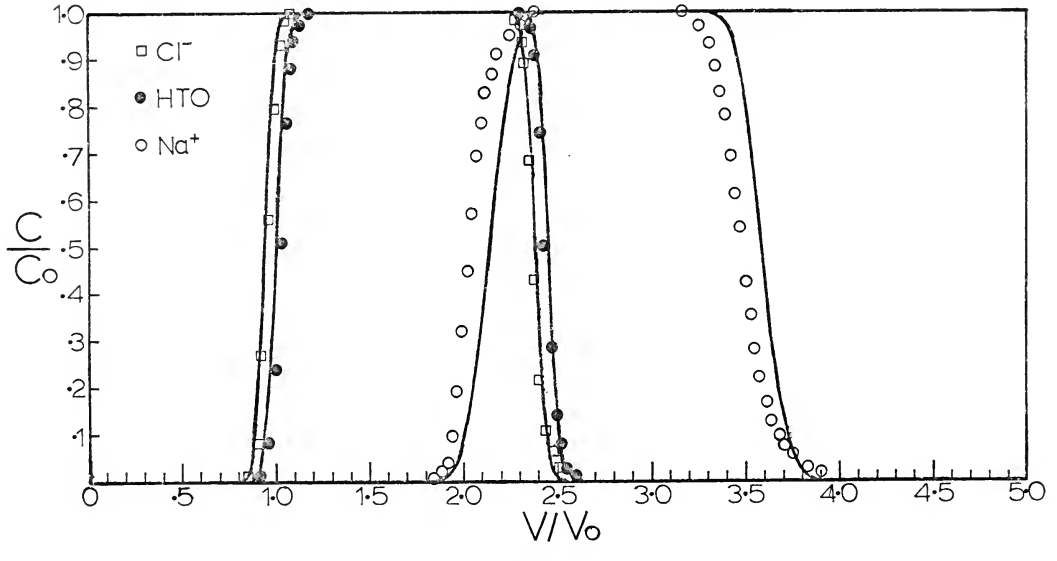

Figure 10. Elution curves for a "pulse input" of Na^+, Cl^-, and HTO in 0.02 M $Ca(NO_3)_2$ at a pore-water velocity between 7 and 8 cm/hr. Solid lines were calculated using equation (45).

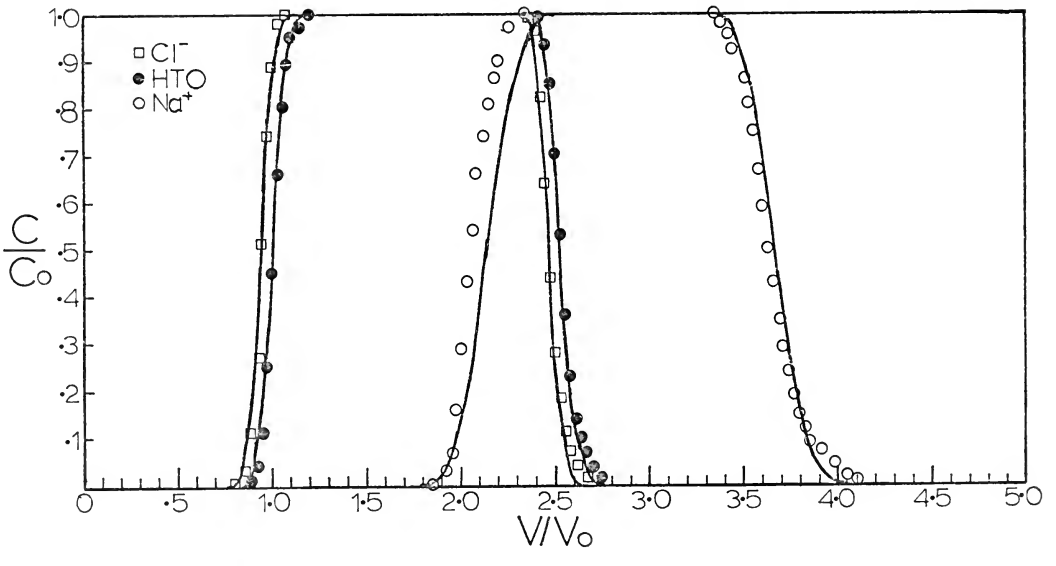

Figure 11. Elution curves for a "pulse input" of Na^+, Cl^-, and HTO in 0.02 M $Ca(NO_3)_2$ at a pore-water velocity between 1 and 2 cm/hr. Solid lines were calculated using equation (45).

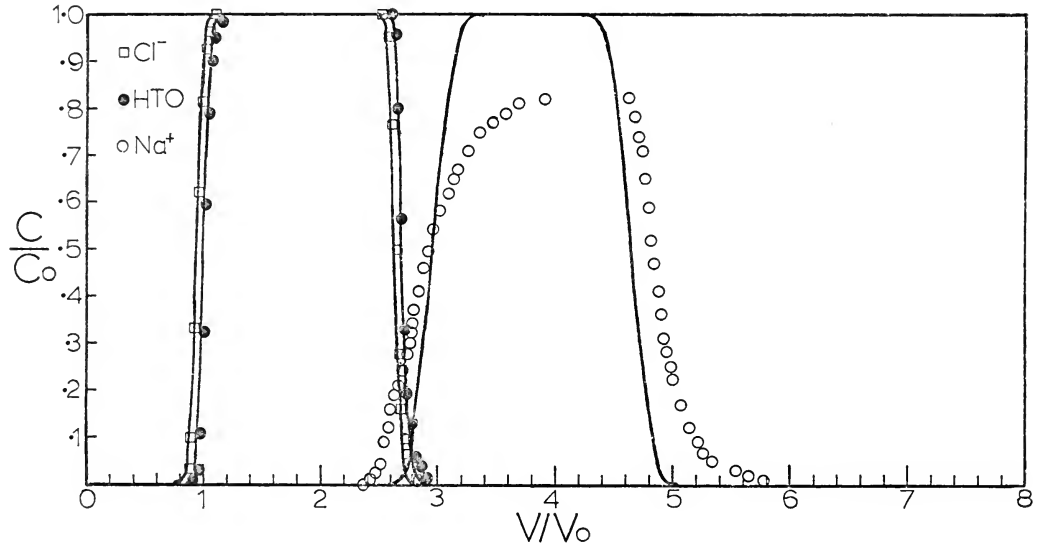

Figure 12. Elution curves for a "pulse input" of Na^+, Cl^-, and HTO in 0.005 N $Ca(NO_3)_2$ at a pore-water velocity between 14 and 15 cm/hr. Solid lines were calculated using equation (45).

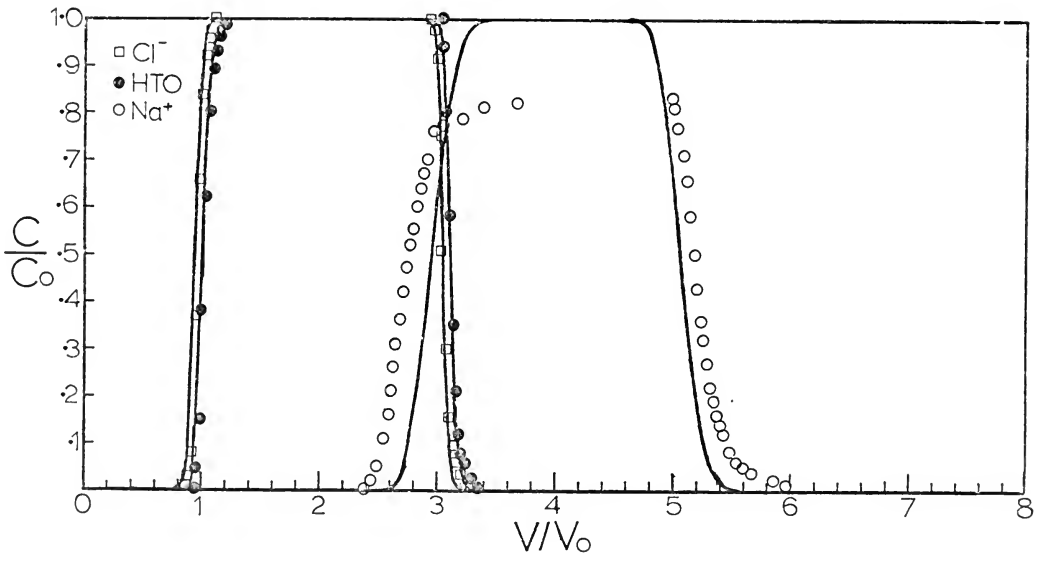

Figure 13. Elution curves for a "pulse input" of Na^+, Cl^-, and HTO in 0.005 M $Ca(NO_3)_2$ at a pore-water velocity between 7 and 8 cm/hr. Solid lines were calculated using equation (45).

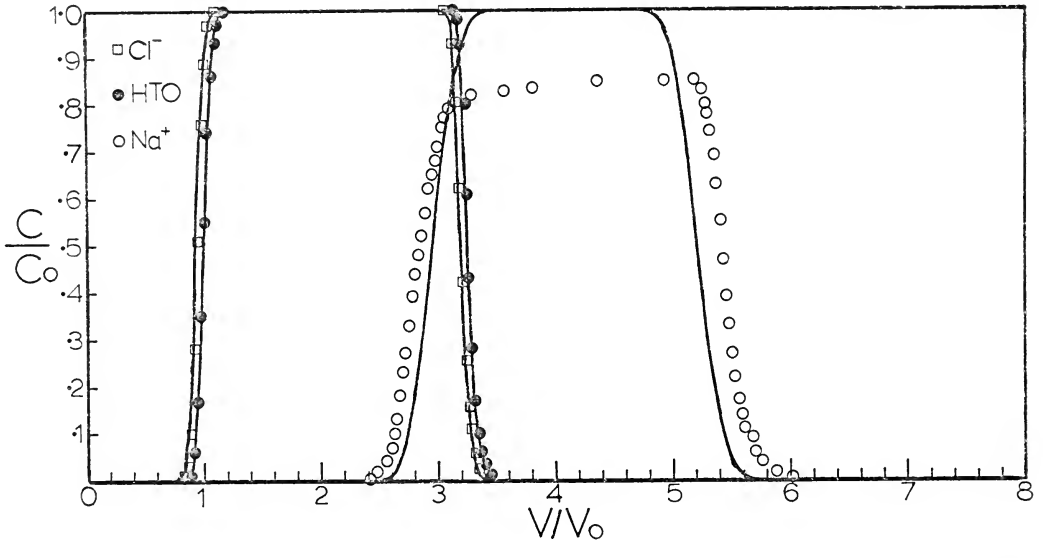

Figure 14. Elution curves for a "pulse input" of Na^+, Cl^-, and HTO in 0.005 M $Ca(NO_3)_2$ at a pore-water velocity between 1 and 2 cm/hr. Solid lines were calculated using equation (45).

the HTO elution curves and were not markedly affected by the $Ca(NO_3)_2$ concentration. The dispersion coefficients averaged over the three $Ca(NO_3)_2$ concentrations and corresponding to the mean pore-water velocity values given above were 0.453 ± 0.025, 0.263 ± 0.040, and 0.082 ± 0.007 cm^2/hr, respectively. These values plotted against the average velocity, as shown in Figure 15, gave a linear relationship. Extrapolation to zero pore-water velocity gave an intercept of 0.0458 cm^2/hr (1.3×10^{-5} cm^2/sec) which represents the diffusion coefficient of HTO. Recent values reported by Mills (51) for the self-diffusion coefficient of HTO are $1.724 \pm 0.003 \times 10^{-5}$ cm^2/sec at 15 C and $2.236 \pm 0.004 \times 10^{-5}$ cm^2/sec at 25 C. The experiments reported in this study were conducted at approximately 20 C. A linear interpolation yields a value of 1.88×10^{-5} cm^2/sec which compares favorably with the experimental value when tortuosity factors are considered.

The elution curves for Cl^- appeared, in all cases, slightly to the left of those for HTO confirming the expected exclusion of Cl^- by the exchanger. Because no exclusion isotherm was measured for Cl^-, the excluded volumes determined by the magnitude of the left-hand shift of the Cl^- curve from $C/C_o = 0.5$ at $V = V_o$ for these nine elution curves were averaged. The excluded volume was calculated to be 12.8 cm^3 using the Cl^- data. This information was used to calculate a "retardation" coefficient of R = 0.938 for Cl^- from the relationship $R = 1 - 12.8/V_o$. As shown in the figures 6 through 14 this value gave analytical curves which described the elution curves for Cl^-.

Analytical curves for Na^+, utilizing R values $(1 + \frac{\rho K}{\theta v})$ calculated with the K values from the appropriate isotherms, described the elution curves for Na^+ in 0.05 M and 0.02 M $Ca(NO_3)_2$ reasonably well. These

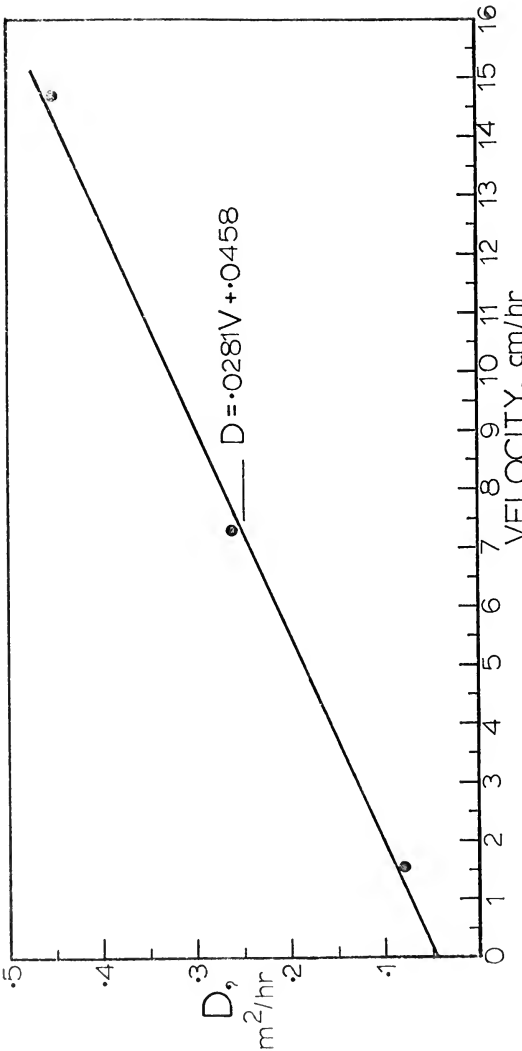

Figure 15. Linear dependence of the dispersion coefficient on the pore-water velocity.

results indicate that equilibrium was instantaneous and followed the experimental isotherm. The somewhat poorer agreement between the analytical and experimental curves for Na^+ in 0.02 M $Ca(NO_3)_2$ was probably the result, in this case only, of not using the same batch of 0.02 M $Ca(NO_3)_2$ solution as that used to determine the adsorption isotherm. Concentration differences between the two batches would explain the consistent left displacements observed in this case. It also underscores the sensitivity of the system to changes in the concentration of Ca^{2+}.

The linear equilibrium model failed completely to describe the elution curves for Na^+ in 0.005 M $Ca(NO_3)_2$. This was unexpected and the displacements in 0.05 M and 0.005 M $Ca(NO_3)_2$ were repeated using a shorter column with ρ = 1.764 g/cm^3 and θ_v = 0.344. These elution curves are presented in Figure 16 and are shown to behave in an identical manner as that observed for the longer column. This rules out the possibility that the observed results were experimental artifacts.

Failure of the equilibrium model to describe experimental data is usually construed as an indication of non-equilibrium. As previously discussed, it was expected that, at the concentrations of Na^+ used, film diffusion would constitute the main resistance to mass transfer. According to this concept, a stagnant fluid film is thought to exist around the exchanger particles across which interphase mass transfer takes place by molecular diffusion. The thickness of this film would vary inversely with fluid velocity. However, no marked shifts or changes were observed in the shapes of the elution curves for Na^+ or HTO in 0.05 M, 0.02 M or 0.005 M $Ca(NO_3)_2$ although the pore velocity was varied by almost an order of magnitude.

Pulse (0.05 M) = 2.265 pv v (0.05 M) = 7.615 cm/hr D (0.05 M) = 0.615 cm^2/hr L = 20.5 cm
Pulse (0.005 M) = 2.258 pv v (0.005 M) = 7.337 cm/hr D (0.005 M) = 0.570 cm^2/hr

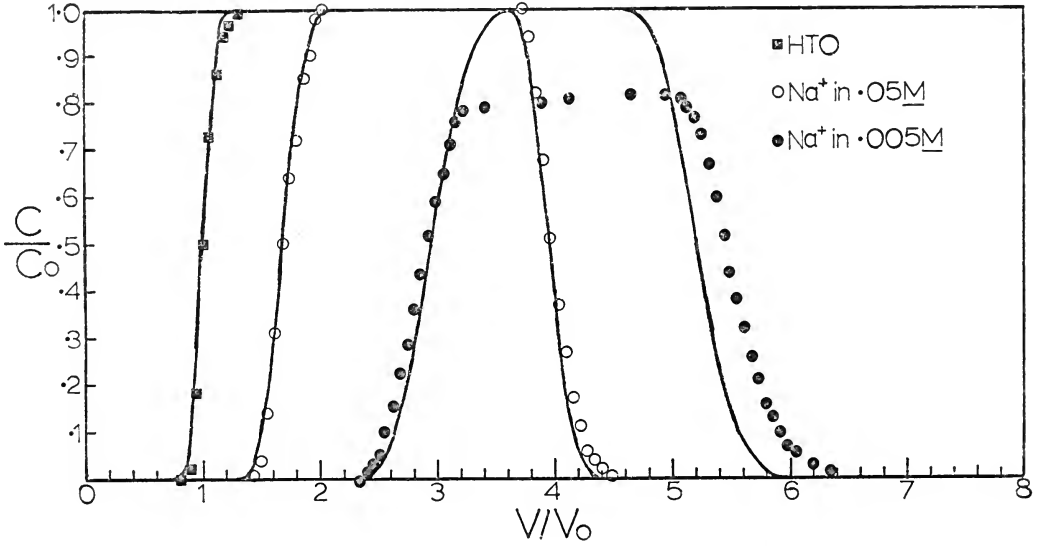

Figure 16. Repeated elution curves for "pulse inputs" of Na^+ and HTO in 0.05 M and 0.005 M $Ca(NO_3)_2$ in a short column at pore-water velocities between 7 and 8 cm/hr. Solid lines were calculated using equation (45).

Whatever the process associated with the observed results in Figure 16, it clearly depends in some fashion upon the concentration of Ca^{2+} in the system, since the concentration of Na^{+} was held constant at 80 - 85 ppm in all cases. The theoretical and experimental studies of Helfferich and his coworkers, reviewed previously, indicated that the interdiffusion coefficient of Na^{+} in either phase would depend upon the relative concentrations of Na^{+} and Ca^{2+} in that phase [equation (26)]. Their theory showed that at low Na^{+} to Ca^{2+} ratios, the interdiffusion coefficient is close to the diffusion coefficient of Na^{+} and approaches that of Ca^{2+} as the ratio increases. However, it was inconceivable that the diffusion coefficients of Na^{+} and Ca^{2+} differed by an amount large enough to account for the drastic changes in the elution curves observed when the concentration of Ca^{2+} was decreased from 0.02 M to 0.005 M. This argument coupled with the observed null effect of variations in pore velocity leads to the conclusion that interdiffusion in films, as conceived above, was not the process responsible for the observed behavior.

The possibility existed that intra-particle diffusion may be the factor responsible for the results presented in Figures 12 to 14. However, if this were true, it was difficult to explain why such results appear only during the displacement of Na^{+} in 0.005 M $Ca(NO_3)_2$ and not with the two higher concentrations. In order to investigate the resistance to intra-particle mass transfer of the exchanger particles, unsulphonated, spherical, 20 - 50 mesh, macroporous copolymer beads were used. Their mean diameter was at least 5 times larger than that of the sulphonated exchanger particles used in the previous experiments. The identical tracer solution of Na^{+} in 0.005 M $Ca(NO_3)_2$

was displaced through a 20.5-cm long column packed with these beads. The elution curves for Cl^-, HTO and Na^+ are shown in Figure 17. These curves showed no indication of diffusional mass-transfer processes thus negating the possibility that intraparticle diffusion kinetics were responsible for the previously observed results. The results in Figure 17 also confirm the assumption that a low resistance to intraparticle mass transfer existed for the macroporous, polystyrene exchanger materials.

From the foregoing studies, it was now clear that diffusional mass transfer kinetics was not the major factor responsible for the failure of the equilibrium model to fit the elution data for Na^+ in 0.005 M $Ca(NO_3)_2$. Experiments for the transport of Li^+ were next used in an effort to gain a deeper insight and provide a reasonable explanation to this anomaly.

Before proceeding onto these experiments, displacements of two tracer pulses consisting of Na^+, Cl^- and HTO in 0.05 M and 0.02 M $Ca(NO_3)_2$ were done for steady-state unsaturated flow conditions in the same column used in the foregoing experiments. The column was kept under a constant pressure of 23 cm of water using the method described previously. The fractional volumetric water content, θ_v, was reduced to 0.2740. The column was positioned vertically in order to give the highest possible flow rate without incurring large water-content gradients in the column. The flow rate was adjusted so that a constant pressure head of 5 - 6 cm of water was maintained at the inlet.

The elution curves for these displacements are presented in Figures 18 and 19. Areas under these curves by the trapezoid rule integration indicated that the material injected with the pulse was

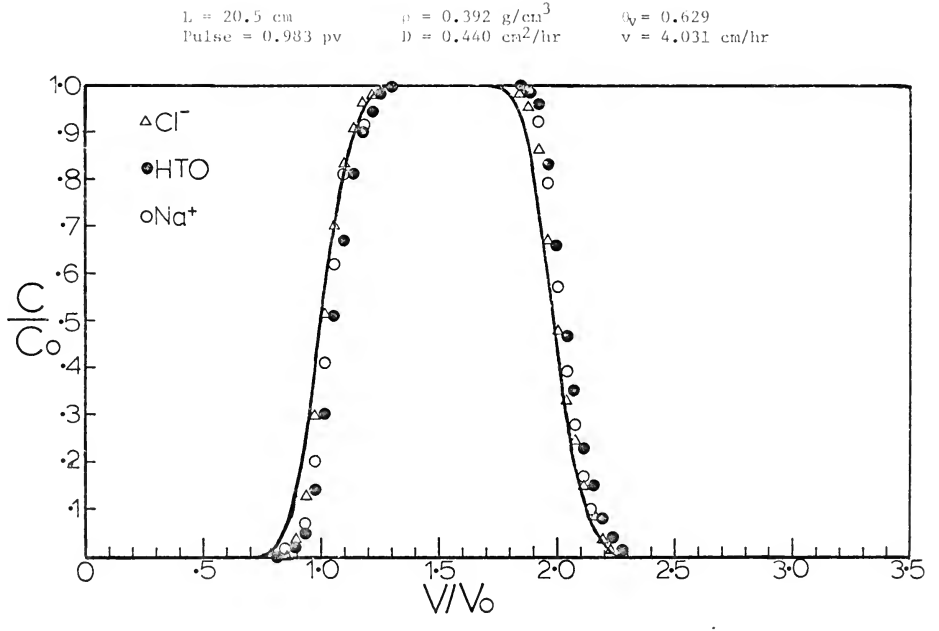

Figure 17. Elution curves for a "pulse input" of Na^+, Cl^-, and HTO in 0.005 M $Ca(NO_3)_2$ in a column packed with unsulphonated, macroporous, polystyrene beads. The solid line represents the analytical curve for a non-reactive solute.

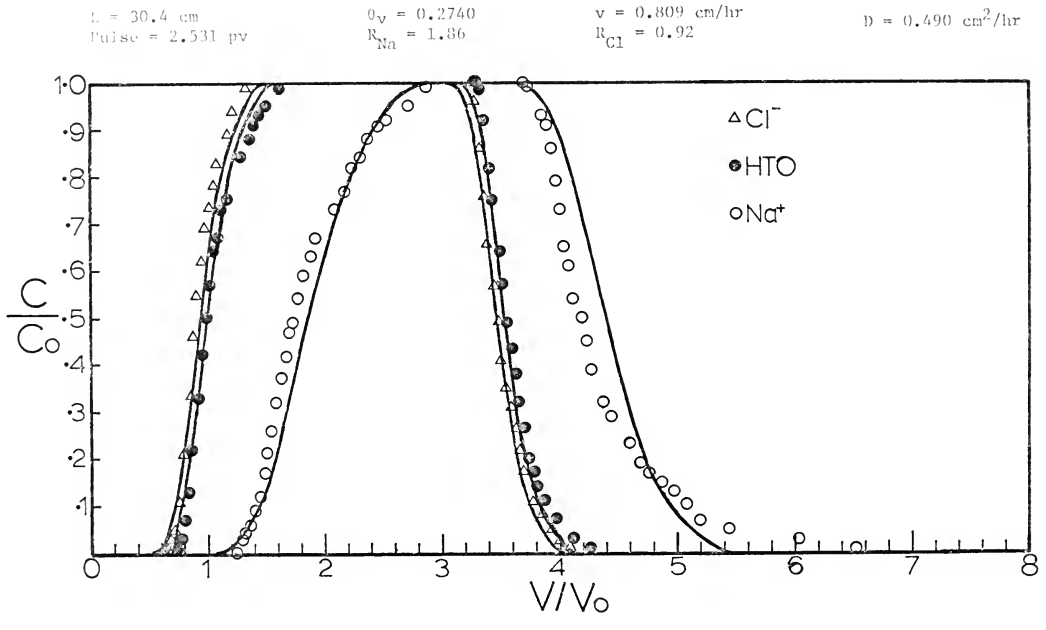

Figure 18. Elution curves for a "pulse input" of Na^+, Cl^-, and HTO in 0.05 M $Ca(NO_3)_2$ under steady-state unsaturated water flow conditions. The solid lines were calculated using equation (45).

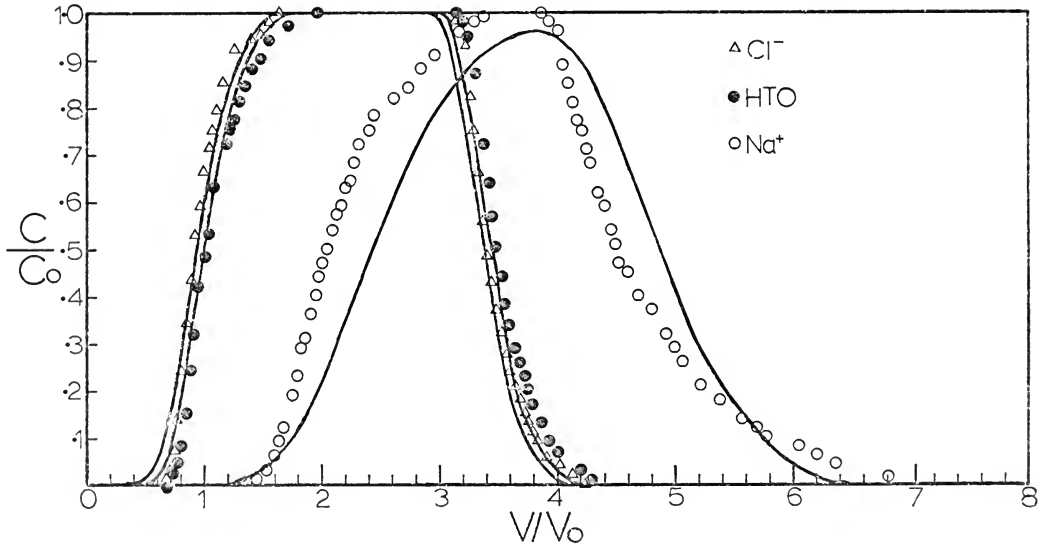

Figure 19. Elution curves for a "pulse input" of Na^+, Cl^-, and HTO in 0.02 M $Ca(NO_3)_2$ under steady-state unsaturated water flow conditions. The solid lines were calculated using equation (45).

recovered completely in the effluent. The R values used for the saturated flow experiments were suitably modified to take into account the reduction in θ_v. The equilibrium model [equation (45)] was used to generate the analytical curves shown in Figures 18 and 19.

Rather poor agreement was obtained between the analytical and experimental curves for Na^+ in 0.05 M $Ca(NO_3)_2$ and was worse for Na^+ in 0.02 M $Ca(NO_3)_2$. The general tendency was a displacement of the experimental data to the left of the predicted analytical curve. It is clear that better agreement is obtained if a lower R value were used. It is possible that with unsaturation a portion of the porous matrix becomes either inaccessible or was accessible only at an extremely slow rate. Subtle arguments are required to justify a shift to the left of the predicted equilibrium curve in the second case. These fortunately were discussed elsewhere (69, 70) and are not presented here because it was the intention of this study to make only cursory observations of Na^+ transport under unsaturated flow conditions.

Miscible Displacement Experiments with Li^+

As a consequence of the foregoing results, it was decided to observe the elution behavior of pulse inputs of Li^+ and HTO in 0.05 M, 0.02 M, and 0.005 M $Ca(NO_3)_2$ at a single fluid pore velocity. The experimental and analytical curves for these displacements are presented in Figures 20, 21, and 22, respectively. Areas under these curves by the trapezoid rule indicated complete recovery of materials injected with the pulse. A 20.5-cm long column packed to a bulk density (ρ) of 1.764 g/cm^3 and with a fractional volumetric water content (θ_v) of 0.344, was used in these and all subsequent displacements involving Li^+.

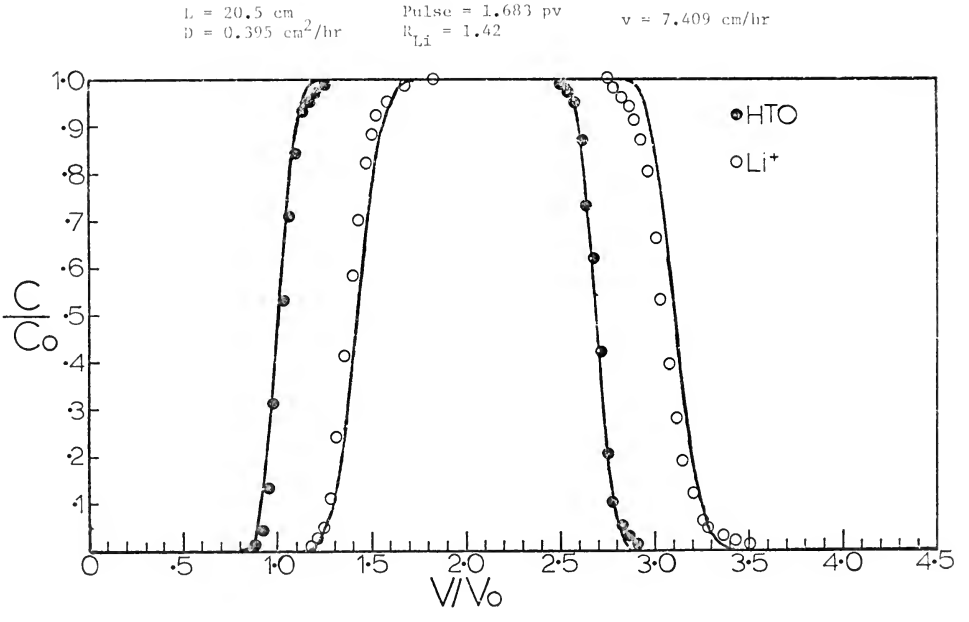

Figure 20. Elution curves for a "pulse input" of Li^+ and HTO in 0.05 M $Ca(NO_3)_2$ at a pore-water velocity between 7 and 8 cm/hr. The solid lines were calculated using equation (45).

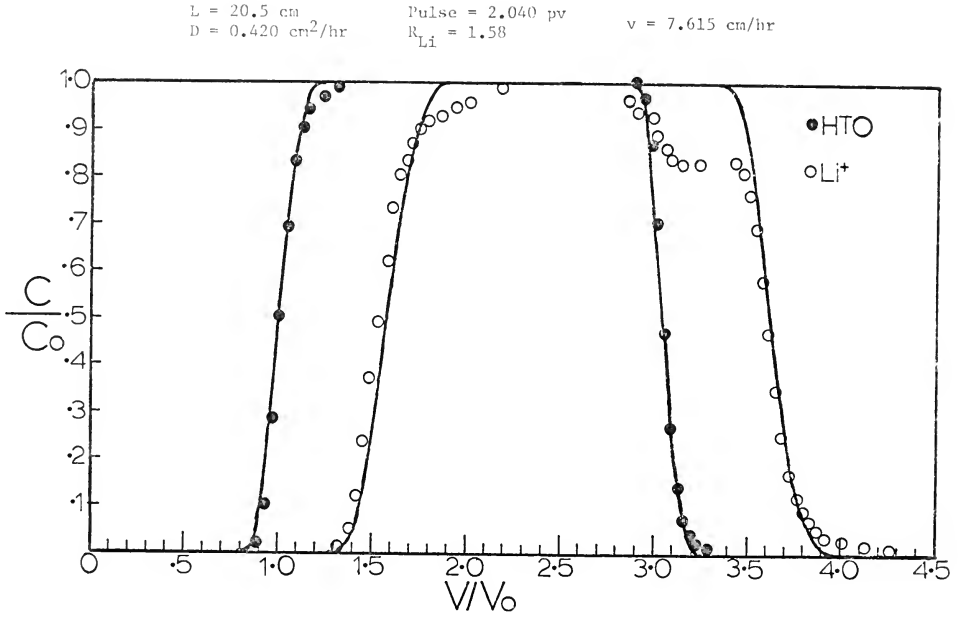

Figure 21. Elution curves for a "pulse input" of Li^+ and HTO in 0.02 M $Ca(NO_3)_2$ at a pore-water velocity between 7 and 8 cm/hr and without adjustment of the ionic strength of the eluting solution. Solid lines were calculated using equation (45).

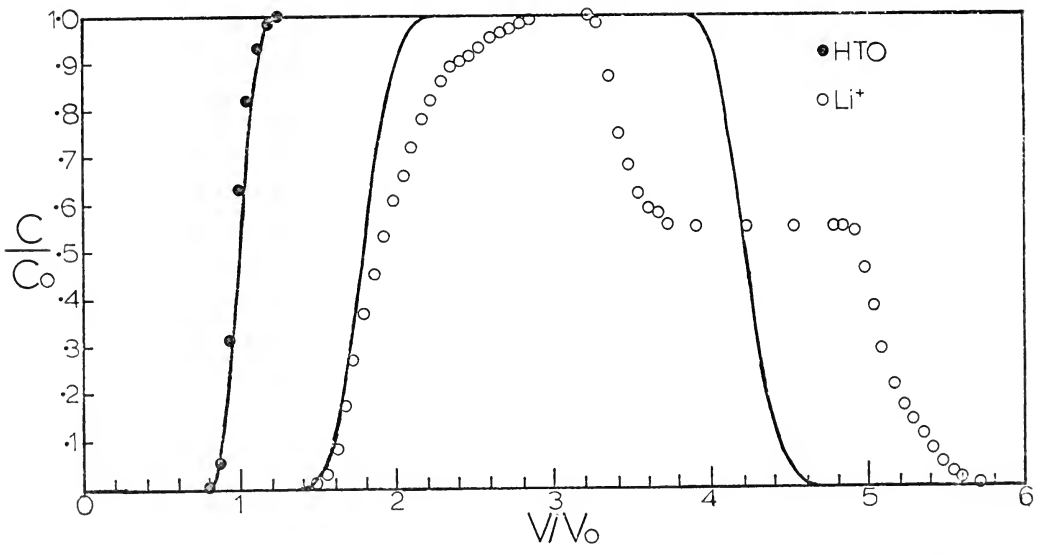

Figure 22. Elution curves for a "pulse input" of Li^+ and HTO in 0.005 M $Ca(NO_3)_2$ at a pore-water velocity between 7 and 8 cm/hr and without adjustment of the ionic strength of the eluting solution. Solid lines were calculated using equation (45).

The behavior of Li^+ in 0.05 M $Ca(NO_3)_2$ agreed with the theoretical curve, but the linear equilibrium model failed to describe the elution patterns of Li^+ in 0.02 M and 0.005 M $Ca(NO_3)_2$. A mild discrepancy was apparent in the front portions of these latter curves becoming more pronounced as the Ca^{2+} concentration was decreased. In order to obtain a concentration of 80 - 85 ppm Li^+ in the tracer solution, it was necessary to add 12.5 cm^3 of 1 M LiCl/liter of tracer solution. This resulted in density differences and may have caused the observed discrepancies which were similar to those reported by Rose and Passioura (62).

The results on the back side of the breakthrough data were in disagreement with the predicted analytical curves. A clue to the reason for this anomalous behavior was provided by the observation that the deviations commenced at approximately one pore volume after changeover to the tracer free eluting solution.

As discussed above, for analytical purposes, it was necessary to keep the concentration of Li^+ in the tracer solutions between 80 - 85 ppm. This concentration of Li^+ resulted in a larger numerical contribution to the ionic strength of these solutions than the same concentration of Na^+. It was, therefore, reasonable to assume that differences in ionic strengths between the eluting and tracer solutions were the reason for the observed behavior. Figures 23 and 24 present elution curves for the displacement of the same tracer solutions of Li^+ in 0.02 M and 0.005 M $Ca(NO_3)_2$, but with the ionic strength of the eluting solution adjusted to match that of the Li^+ plus $Ca(NO_3)_2$ tracer solution. The observed inflections in both cases were altered, but did not disappear completely; however, the change was towards better agreement

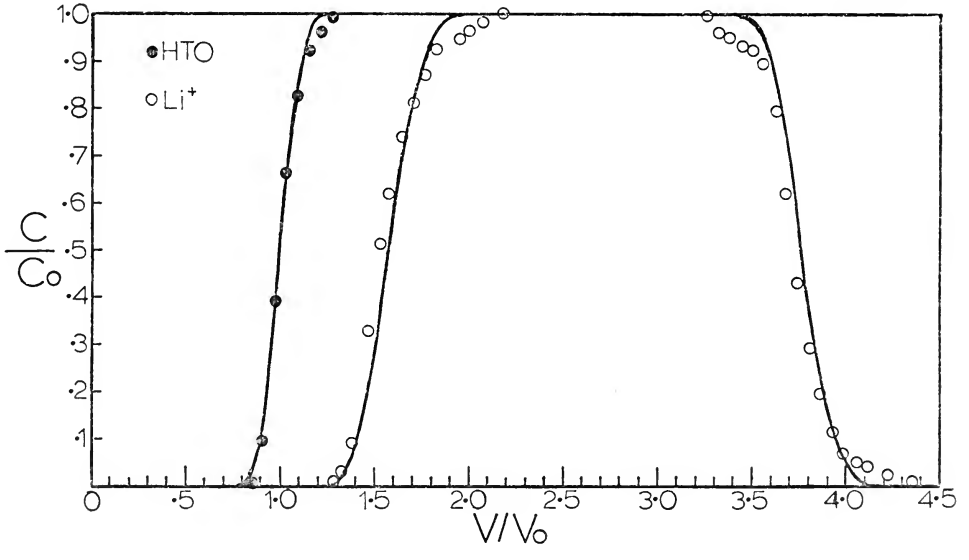

Figure 23. Elution curves for a "pulse input" of Li^+ and HTO in 0.02 M $Ca(NO_3)_2$ at a pore-water velocity between 7 and 8 cm/hr and with adjustment of the ionic strength of the eluting solution. Solid lines were calculated using equation (45).

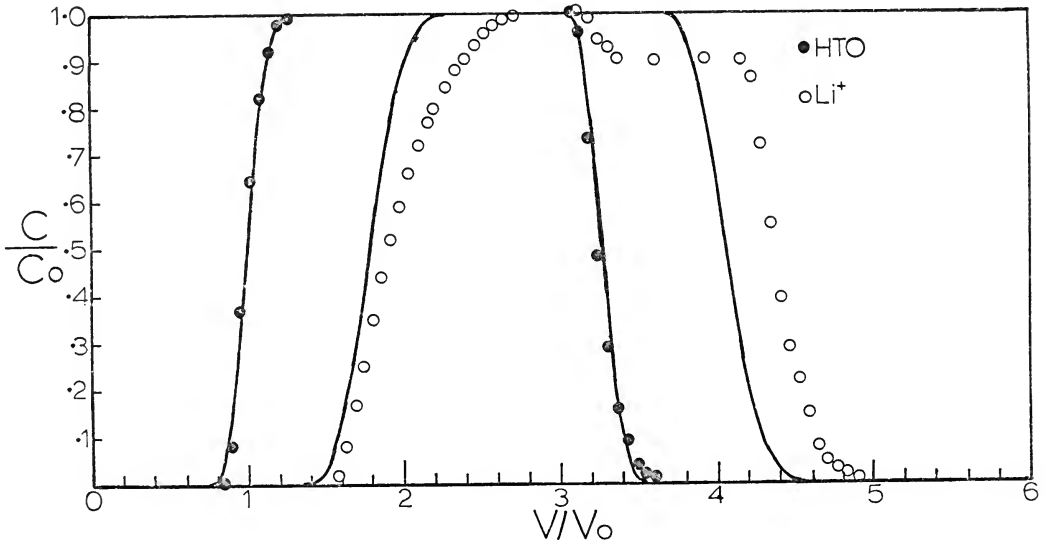

Figure 24. Elution curves for a "pulse input" of Li^+ and HTO in 0.005 M $Ca(NO_3)_2$ at a pore-water velocity between 7 and 8 cm/hr and with adjustment of the ionic strength of the eluting solution. Solid lines were calculated using equation (45).

with the calculated curves. In order to pursue this idea further and to confirm that the concentration of Li^+ was a contributing factor, displacements were conducted using 50 - 55 ppm Li^+ in 0.02 M $Ca(NO_3)_2$ and 0.01 M $Ca(NO_3)_2$. These elution curves are shown in Figure 25. The analytical curves were generated using a value of D obtained from a previous displacement at almost the same pore-water velocity. The R value for the displacement of Li^+ at 50 - 55 ppm in 0.01 M $Ca(NO_3)_2$ was computed using the empirical exponential relationship for the dependence of K on the concentration of Ca^{2+} (Figure 4). The inflection in the elution curve for the displacement of Li^+ in 0.02 M $Ca(NO_3)_2$ was less pronounced than for the displacement of Li^+ at 80 - 85 ppm. The inflection in the elution curve for the displacement in 0.01 M $Ca(NO_3)_2$ was more pronounced than in 0.02 M $Ca(NO_3)_2$; showing similar enhancement with decreasing Ca^{2+} concentrations as those observed previously (Figures 21 and 22).

The foregoing experiments served to isolate some factors associated with the observed results, but did not provide any insight into the mechanism. This was needed to explain why the effect appeared only on the desorption portions of the elution curves and why the inflections did not disappear with ionic strength corrections. In addition, calculations utilizing the extended Debye-Hückel formula show that the activity of Ca^{2+} in the tracer solutions containing 80 - 85 ppm Li^+ in 0.05 M, 0.02 M and 0.005 M $Ca(NO_3)_2$ were respectively 2.4, 4.8 and 11.4% less than the corresponding activities in the pure solutions. It was shown above [equation (48c)] that the K value is inversely related to the activity of Ca^{2+}. The above results therefore imply a depression in adsorption with a resulting increase instead of a decrease in the Li^+ concentration of the solution phase.

Pulse (0.02 M) = 2.313 pv v (0.02 M) = 7.470 cm/hr R_{Li} (0.02 M) = 1.58 D = 0.550 cm^2/hr
Pulse (0.01 M) = 3.031 pv v (0.01 M) = 7.458 cm/hr R_{Li} (0.01 M) = 1.76 L = 20.5 cm

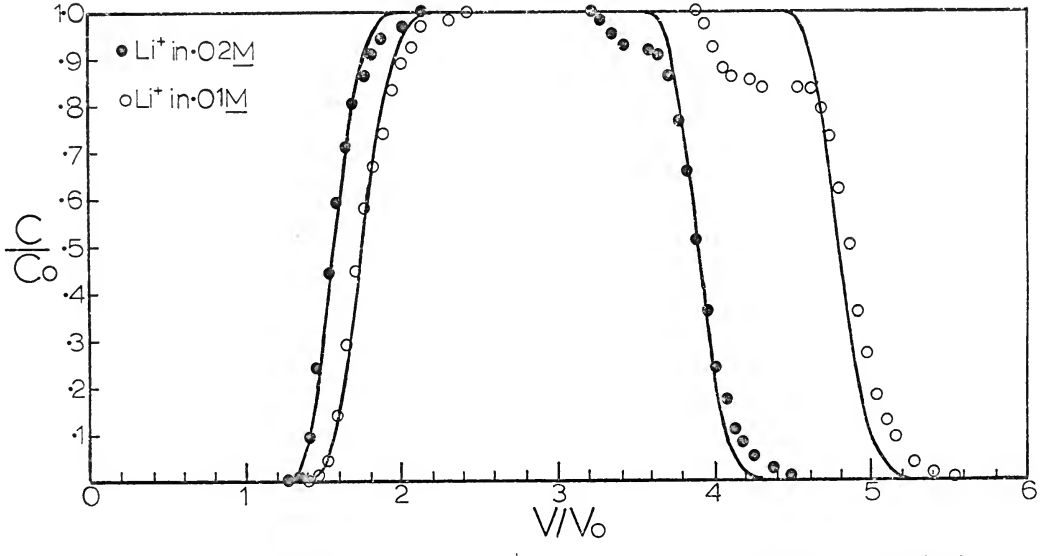

Figure 25. Elution curves for "pulse inputs" of Li^+ at 50 to 55 ppm in 0.02 M and 0.01 M $Ca(NO_3)_2$ at pore-water velocities between 7 and 8 cm/hr and without adjustment of the ionic strength of the eluting solution. The solid lines were calculated using equation (45).

These facts led to the following experiment which provided a reasonable explanation for both the observed inflections and the anomalous behavior of Na^+ in 0.005 M $Ca(NO_3)_2$. The solution in the column was displaced with a tracer solution containing 80 - 85 ppm of Li^+ in 0.005 M $Ca(NO_3)_2$ until the concentration of Li^+ in the effluent was equal to its concentration in the influent solution. This implies that equilibrium was achieved at all points within the system. This solution was then displaced with deionized water and the concentrations of all components in the effluent were monitored. The appearance of Ca^{2+} and Cl^- was monitored qualitatively by precipitation with Na-oxalate and $AgNO_3$, respectively. Nitrate was identified by the brown ring test. At exactly one pore volume, the concentrations of all components including Li^+ fell sharply to zero. It thus became clear that the electroneutrality requirement peculiar to ion exchange adsorption processes resulted in all components behaving as non-reactive solutes once equilibrium was achieved. This result implies that an amount of Li^+ equivalent to $\frac{\rho K}{\theta_v} V_o C_o$ remained adsorbed by the exchanger.

The adsorbed Li^+ was then eluted with a 0.005 M $Ca(NO_3)_2$ solution. The elution curve showed the appearance of Li^+ shortly before one pore volume, rising sharply to a steady maximum concentration and then falling sharply to zero at approximately 2.56 pore volumes. This behavior is analogous to that observed on the back side of the pulse elution data for Li^+ in 0.005 M $Ca(NO_3)_2$ (Figure 22). These results are presented in Figure 26, and indicate that the exchange adsorption for Li^+ in 0.005 M $Ca(NO_3)_2$ was distinct from its exchange desorption. If the same K value characterized both processes, the elution volume for desorption should have been $R_{Li} = 1.79$ pore volumes instead of observed

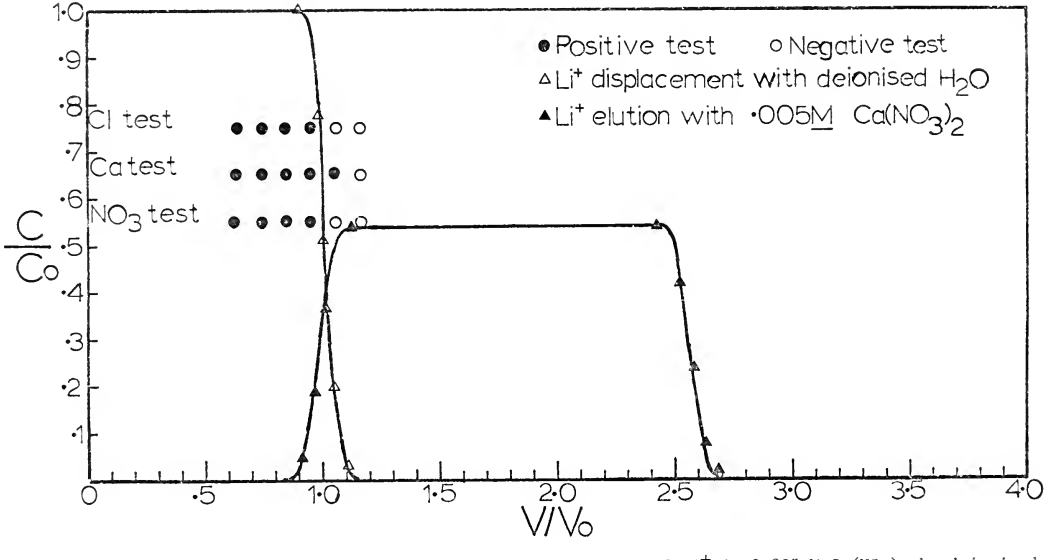

Figure 26. Observations on the elution pattern for displacement of Li^+ in 0.005 M $Ca(NO_3)_2$ by deionized H_2O followed by 0.005 M $Ca(NO_3)_2$.

value of 2.56. This indicates that a higher K value was associated with the desorption process.

The samples collected from the desorption experiment were tested for Ca^{2+} with Na-oxalate solution. The tests showed that Ca^{2+} appeared in the effluent with the Li^{+}. It was also observed by comparing the turbidity developed in the effluent samples with a standard (0.005 M $Ca(NO_3)_2$) that the concentration of Ca^{2+} rose sharply to a maximum concentration which was less than 0.005 M. The Ca^{2+} concentration remained at the lower level until the elution of Li^{+} was complete, after which it rose to 0.005 M. This was expected because electo-neutrality necessitates that an equivalent amount of Ca^{2+} replace the Li^{+} desorbed. These results indicate that the desorption of Li^{+} occurs with a concentration of Ca^{2+} in the solution phase less than 0.005 M. This implies a lower Ca^{2+} activity and therefore a higher K value [Equation (48c)].

The concentration of Li^{+} in the saturating solution was 0.0122 M and from the exchange desorption curve the maximum value reached was 0.0067 M. Applying the electroneutrality requirement, the concentration of Ca^{2+} would have to decrease from 0.005 M to 0.0016 M. Thus, during desorption the solution phase constitution is Li^{+} = 0.0067 M, Ca^{2+} = 0.0016 M, NO_3^{-} = 0.01 M. This yields a value for the ionic strength of 0.0117 M. With this value the extended Debye-Hückel formula gives values for γ_{Li} = 0.9012 and $\sqrt{a}_{Ca}$ = 0.0325. The empirical formula $K = \gamma_{Li}/70.183\ \sqrt{a}_{Ca}$, used previously to calculate K values of the adsorption isotherms for Li^{+}, yields a value of K = 0.3952 which gives $\frac{\rho K}{\theta_v}$ = 2.03. This value is greater than the experimental value of 1.56 (Figure 26) but it is in the right direction. Observations from the

elution curve for Li^+ in 0.02 M $Ca(NO_3)_2$ given in Figure 21 suggest that if a similar experiment as that described above were conducted with 0.02 M $Ca(NO_3)_2$, a maximum concentration of $Li^+ = 0.82\ C_o$ would result for the desorption process. By the same reasoning, the concentration of the various species in the solution phase would be $Li^+ = 0.01$ M, $Ca^{2+} = 0.015$ M, $NO_3^- = 0.04$ M yielding an ionic strength of 0.055 M. Similar calculations yield values of $\gamma_{Li} = 0.8292$, $\sqrt{a}_{Ca} = 0.0842$, a predicted K value of 0.1403, and $\frac{\rho K}{\theta_v} = 0.7205$. The value of $\frac{\rho K}{\theta_v}$ compares favorably with the observed value of 0.60 (Figure 21).

The inflections observed in the elution curves for Li^+ (Figures 21 through 25) become clear in light of the above results. When lower concentrations of $Ca(NO_3)_2$ were used in the tracer pulse, the quantity of Li^+ adsorbed is increased. The desorption process is characterized by a K value that is dependent on the activity coefficient of Li^+ and the activity of Ca^{2+} in the desorbing solution. If a low concentration of $Ca(NO_3)_2$ was used in this solution, the equivalence of exchange results in a reduced value for the activity of Ca^{2+} and hence a correspondingly larger K value. When the concentration of the desorbing $Ca(NO_3)_2$ solution is increased, the K value decreases. In addition, at higher concentrations of $Ca(NO_3)_2$, the effect of the adsorption of Ca^{2+} would be less pronounced. The desorption K value then approaches more closely the K value for adsorption. These facts explain the reduced degree of inflection when the concentration of the eluting $Ca(NO_3)_2$ was increased to match the ionic strength of the tracer solution, or when the concentration of Li^+ in the latter was lowered. In addition, it explains why the inflections did not disappear after the ionic strength adjustment and why they were not observed for the displacement of Li^+ in 0.05 M $Ca(NO_3)_2$.

The foregoing results also clarify the apparent kinetic effect observed for displacements of Na^+ in 0.005 N $Ca(NO_3)_2$. Examination of the condition under which the data in Figures 11 through 14 were obtained reveals that because of large R values, the tracer front for Na^+, in all cases, had not reached the Covalue in the effluent at the time of changeover to the eluting solution. It is obvious from the foregoing that this would result in a change in the ionic composition of the solution phase before the column was completely equilibrated with Na^+. Thus, instead of reaching a maximum concentration of Co, the effluent would reach a maximum lower than Co. This idea was tested by a step input displacement experiment with Na^+ in 0.005 M $Ca(NO_3)_2$. The result given in Figure 27 shows that the above is indeed a reasonable explanation since the effluent now shows none of the previous apparent kinetic effect. A further point in favor of the correctness of this hypothesis is that it explains why the apparent kinetic effect was associated with only the front portion of the curves. If true kinetic processes were operating and the adsorption isotherm was linear the effect would have been symmetrical.

In light of the foregoing, the data for Na^+ in 0.02 N $Ca(NO_3)_2$ may seem anomalous since they did not show inflections. It is likely that inflections such as those for Li^+ in 0.02 N $Ca(NO_3)_2$ may have existed but were overlooked because they were too small.

Miscible Displacement Experiments with $^{45}Ca^{2+}$

Two displacements of pulse inputs were conducted with $^{45}Ca^{2+}$ in 0.05 N and 0.075 N $Ca(NO_3)_2$ to verify that the adsorption isotherms for $^{45}Ca^{2+}$ do reflect appropriately in their transport behavior. Because of large R values, these displacements were conducted in a shorter

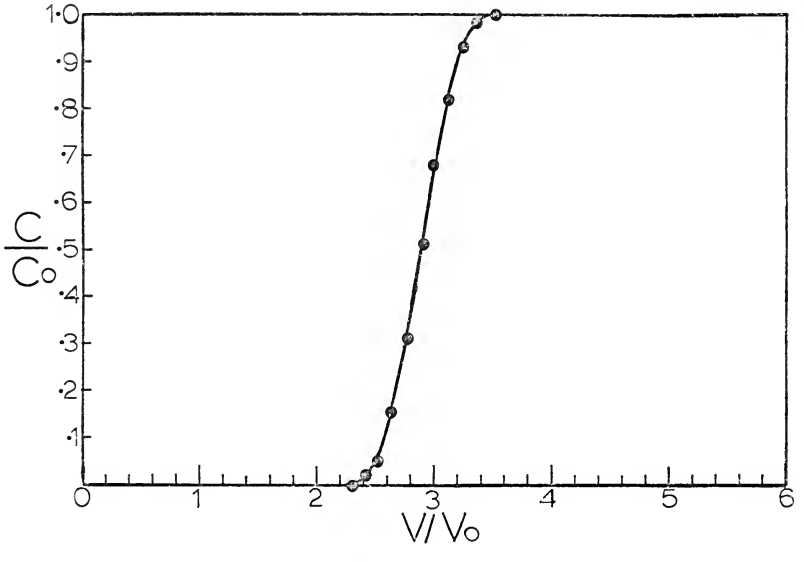

Figure 27. Breakthrough curve for a "step input" of Na^+ in 0.005 M $Ca(NO_3)_2$.

5.7-cm long column packed to a bulk density (ρ) of 1.769 g/cm^3 and saturated to a fractional volumetric water content (θ_v) of 0.347.

The results of these displacements are given in Figure 28. Because of the shorter column, experimental error was greater. In both cases, if higher R values were used, closer agreement would have been obtained between the experimental and analytical curves.

It is interesting to observe that for the displacement in 0.05 M $Ca(NO_3)_2$ changeover to the eluting solution before the tracer front had completely appeared in the effluent, resulted in a similar disagreement between the analytical and experimental curve as was obtained for Na^+ in 0.005 M $Ca(NO_3)_2$. Further, the use of a much larger pulse for the displacement in 0.075 M $Ca(NO_3)_2$ produced the expected inflection at approximately one pore volume after changeover and a shift to the right of the analytical curve.

These results confirm that the behavior of Na^+ in 0.005 M $Ca(NO_3)_2$ cannot be attributed to the effect of relative concentrations of Na^+ to Ca^{2+} on the interdiffusion coefficient of either ion. Examination of the relevant equation of Helfferich and his coworkers [equation (26)], reveals that in the case of isotopic exchange, the interdiffusion coefficient is equal to the diffusion coefficient of Ca^{2+} and independent of relative concentrations. Also, increasing the relative concentration of Na^+ to Ca^{2+} should result in the interdiffusion coefficient approaching the diffusion coefficient of Ca^{2+}. If this were indeed responsible for the behavior of Na^+ in 0.005 M $Ca(NO_3)_2$, then similar effects should have appeared in both the elution curves for $^{45}Ca^{2+}$. This however was not observed.

L = 5.7 cm

v (HTO) = 6.665 cm/hr
v (0.075 M) = 7.618 cm/hr
v (0.05 M) = 7.130 cm/hr

Pulse (HTO) = 1.747 pv
Pulse (0.075 M) = 11.508 pv
Pulse (0.05 M) = 6.484 pv

D = 0.650 cm^2/hr
R (0.075 M) = 4.89
R (0.05 M) = 6.31

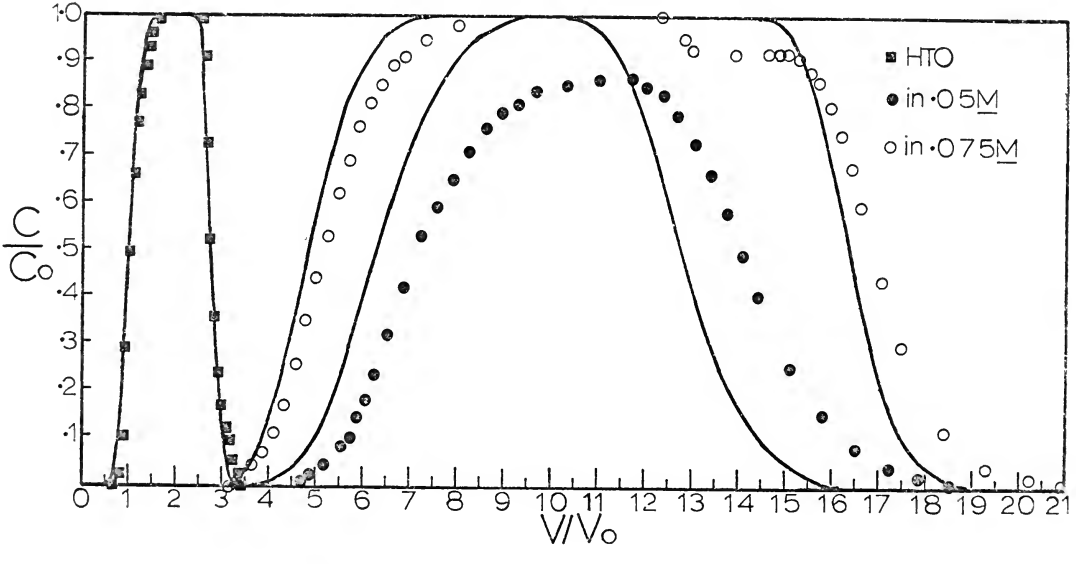

Figure 28. Elution curves for "pulse inputs" of HTO and $^{45}Ca^{2+}$ in 0.075 M and 0.05 M $Ca(NO_3)_2$. Solid lines were calculated using equation (45).

CHAPTER 6

SUMMARY AND CONCLUSIONS

Theoretical approaches to describe cation exchange processes are fairly recent although the topic spans a period of over a century. Despite the acknowledged importance of this process in soil systems, there are only a few references which deal with transport of ionic species. In this study, the miscible displacement technique was utilized to investigate the influence of exchange adsorption on the transport of selected inorganic ions in a porous medium. The influence of dispersion and exclusion was also studied. A Ca-saturated organic cation exchanger was used as the medium, which eliminated the possibility of interactions other than ion exchange.

Solution and exchanger was conceived as a heterogeneous system consisting of two mixed phases. A thermodynamic treatment based on this concept predicted the exclusion of anions. It was shown that, in general, solution-phase ions common to those initially saturating the exchanger influence the adsorption of other charged species. This was adequately verified by experimental exchange adsorption isotherms determined for Na^+ and Li^+ in 0.05 M, 0.02 M and 0.005 M $Ca(NO_3)_2$ and for $^{45}Ca^{2+}$ in 0.075 M and 0.05 M $Ca(NO_3)_2$. For the range of concentrations studied, the adsorption isotherms for Li^+ and Na^+ were linear and their slopes increased in a non-linear fashion with decreasing Ca^{2+} concentration in the equilibrium solutions. Similar trends were evident from the $^{45}Ca^{2+}$ exchange isotherms. It was demonstrated inductively

that these results could be attributed to ion-ion interactions as conceived and quantified by the Debye-Huckel theory.

Miscible displacement experiments involving Na^+, Li^+, $^{45}Ca^{2+}$ and Cl^- were conducted to examine the consequences of the foregoing results, and to determine the presence of kinetic mass-transfer processes. All experiments were performed using pulse inputs of the tracer solution. Tritiated water (HTO) was present in all tracer solutions in order to evaluate dispersion. An asymptotic solution to the convective-dispersion transport equation for a reactive solute (linear adsorption isotherm) was used to predict the experimental breakthrough data.

A series of displacements involving pulses of Na^+, HTO, and Cl^- in 0.05 M, 0.02 M or 0.005 M $Ca(NO_3)_2$ were conducted under steady-state water-saturated flow conditions at three pore-water velocities ranging from 1.5 to 15 cm/hr. Dispersion coefficients obtained from the HTO elution data were not influenced by $Ca(NO_3)_2$ concentration and were linearly related to pore-water velocity. The elution curves for Cl^- were all displaced to the left of those for HTO confirming its exclusion by the exchanger. Reasonable agreement was obtained between the computed and experimental elution curves for Na^+ in 0.05 M and 0.02 M $Ca(NO_3)_2$ at all pore-water velocities studied. The analytical solution, however, failed to describe any of the experimental elution curves for Na^+ in 0.005 M $Ca(NO_3)_2$. These results could have been used to support the concept of diffusional mass-transfer kinetics, but it was shown experimentally that such processes were not involved.

A series of similar steady-state, water-saturated column experiments were conducted to study the transport behavior of Li^+ and HTO

in 0.05 M, 0.02 M and 0.005 M $Ca(NO_3)_2$ at pore-water velocities between 7 and 8 cm/hr. The analytical solution described the front portions of the experimental elution curves reasonably well but, except for Li^+ in 0.05 M $Ca(NO_3)_2$, failed to describe the back side of the elution data. Inflections were observed on the back side of the pulse elution data. Further experiments indicated that the severity of these inflections depended upon both the concentration of $Ca(NO_3)_2$ used for the exchange desorption and the concentration of Li^+ in the tracer pulse. These observations resulted in the performance of an experiment in which it was demonstrated that the parameter associated with the exchange adsorption of Li^+ in 0.005 M $Ca(NO_3)_2$ was different from its counterpart during desorption. It was further shown by inductive reasoning that this was true for all cases and was a direct consequence of the metathetical nature of the sorption process. With this conslusion, it was possible to clarify the anomalous and unexplained results observed in the displacement experiments involving Na^+ in 0.005 M $Ca(NO_3)_2$. These concepts were further supported by the data from displacement experiments with $^{45}Ca^{2+}$ in 0.075 M and 0.05 M $Ca(NO_3)_2$.

Displacement experiments were conducted to obtain a preliminary description of the transport behavior of Na^+, Cl^-, and HTO under steady-state unsaturated water-flow conditions. Two experiments were conducted involving pulse inputs containing these species in 0.05 M and 0.02 M $Ca(NO_3)_2$. The exclusion of Cl^- was evident in both experiments. The analytical solution failed to describe the experimental elution

curves of Na^+ in both cases. These cursory observations indicated that unsaturation resulted in portions of the exchanger phase becoming either inaccessible or accessible only by diffusion which is a rate-controlled process.

The foregoing results, viewed in their entirety, show that in general the exchange adsorption isotherm for a cation is a function of the activities of all charged species in both the solution and exchanger phases. In addition, the exchange adsorption process is at all times subject to the electroneutrality restraint, and this results in its metathetical character. These two facts are fundamental to explaining or predicting the transport behavior of cations in reactive media including soils. The physical and chemical properties of soil exchanger materials are somewhat different from those of synthetic exchangers. The applicability of the concepts and relationships utilized in this study, to ion exchange adsorption and transport in soils can be evaluated only by further investigation.

LITERATURE CITED

1. Ames, W. F. 1977. Numerical methods for partial differential equations. Academic Press, New York.

2. Amundson, N. R. 1948. A note on the mathematics of adsorption in beds. J. Phys. Chem. 52:1153-1157.

3. Amundson, N. R. 1950. Mathematics of adsorption in beds II. J. Phys. Chem. 54:812-820.

4. Aronofsky, J. S., and J. P. Heller. 1957. A diffusion model to explain mixing of flowing miscible fluids in porous media. Trans. A. I. M. E. 210:345-349.

5. Bauman, W. C., and J. Eichhorn. 1947. Fundamental properties of a synthetic cation exchange resin. J. Amer. Chem. Soc. 69:2830-2836.

6. Bear, J. 1969. Hydrodynamic dispersion Chap. 4. In Flow through porous media, R. J. M. DeWiest (editor). Academic Press, New York.

7. Bolt, G. H. 1955. Ion adsorption by clays. Soil Sci. 79:267-276.

8. Bolt, G. H. 1955. Analysis of the validity of the Gouy-Chapman theory of the electrical double layer. J. Colloid Sci. 10:206-218.

9. Bonner, O. D. 1954. A selectivity scale for some monovalent cations on Dowex 50. J. Phys. Chem. 58:318-320.

10. Bonner, O. D., and W. H. Payne, 1954. Equilibrium studies of some monovalent ions on Dowex 50. J. Phys. Chem. 58:183-185.

11. Boyd, G. E., J. Schubert, and A. W. Adamson. 1947. The exchange adsorption of ions from aqueous solutions by organic zeolites I. Ion exchange equilibria. J. Amer. Chem Soc. 69:2818-2829.

12. Boyd, G. E., A. W. Adamson, and L. S. Meyers. 1947. The exchange adsorption of ions from aqueous solutions by organic zeolites II. Kinetics. J. Amer. Chem. Soc. 69:2836-2848.

13. Boyd, G. E., and B. A. Soldano. 1954. Self diffusion of cations in and through sulfonated polystyrene cation exchange polymers. J. Amer. Chem. Soc. 75:6091-6099.

14. Brenner, H. 1962. The diffusion model of longitudinal mixing in beds of finite length. Numerical values. Chem. Eng. Sci. 17:229-243.

15. Coats, K. H., and B. D. Smith. 1964. Dead end pore volume and dispersion in porous media. Soc. Petrol. Engrs. Jour. 4(1):73-84.

16. Danckwerts, P. V. 1953. Continuous flow systems - Distribution of residence times. Chem. Eng. Sci. 2:1-17.

17. Davidson, A. W., and W. J. Argersinger. 1953. Equilibrium constants of cation exchange processes. Annals New York Acad. Sci. 57:105-115.

18. Davis, L. E. 1945. Simple kinetic theory of ionic exchange for ions of unequal charge. J. Phys. Chem. 49:473-479.

19. Day, P. R. 1956. Dispersion of a moving salt water boundary advancing through saturated sand. Trans. Amer. Geophys. Union 37(5):595-601.

20. Day, P. R., and W. M. Forsythe. 1957. Hydrodynamic dispersion of solutes in the soil moisture stream. Soil Sci. Soc. Amer. Proc. 21:477-480.

21. Duncan, J. F., and B. A. J. Lister. 1949. Ion exchange studies II. The determination of thermodynamic equilibrium constants. Disc. Faraday Soc. 7:104-114.

22. Eriksson, E. 1952. Cation exchange equilibria on clay minerals. Soil Sci. 74:103-113.

23. Fara, H. D., and A. E. Scheidegger. 1961. Statistical geometry of porous media. Jour. Geophys. Res. 66(10): 3279-3284.

24. Fatt, I., R. C. Goodknight, and W. A. Klikoff. 1960. Non-steady state fluid flow and diffusion in porous media containing deadend pore volume. J. Phys. Chem. 64:1162-1168.

25. Fried, J. J., and M. A. Combarnous. 1971. Dispersion in porous media. Adv. Hydroscience 7:169-282.

26. Gaines, G. L., and H. C. Thomas. 1953. Adsorption studies in clay minerals II. A formulation of the thermodynamics of exchange adsorption. J. Phys. Chem. 21:714-718.

27. Glueckauf, E. 1952. Theoretical treatment of cation exchangers I. Prediction of equilibrium constants from osmotic data. Proc. Roy. Soc. London A 214:207-224.

28. Glueckauf, E. 1955. Theory of chromatography part 9. The theoretical plate concept in column separations. Trans. Faraday Soc. 51:34-44.

29. Glueckauf, E., and J. J. Coates. 1947. Theory of chromatography part IV. The influence of incomplete equilibrium on the front boundary of chromatograms and on the effectiveness of separation. J. Chem. Soc. 100 part 2:1315-1321.

30. Gregor, H. P., and M. H. Gottlieb. 1953. Activity coefficients of diffusible ions in various cation exchange resins. J. Amer. Chem. Soc. 75:3539-3543.

31. Guggenheim, E. A. 1929. The conceptions of the electrical potential difference between two phases and the individual activities of ions. J. Phys. Chem. 33:842-849.

32. Hale, D. K., and D. Reichenberg. 1949. Equilibrium and rate studies of cation exchange with monofunctional resins. Disc. Faraday Soc. 7:79-90.

33. Haring, R. E., and R. A. Greenkorn. 1970. A statistical model of a porous medium with non-uniform pores. Amer. Inst. Chem. Engrs. Jour. 16:477-483.

34. Helfferich, F. 1962. Ion exchange kinetics III. Experimental test of the theory of particle-diffusion controlled ion exchange. J. Phys. Chem. 66: 39-44.

35. Helfferich, F. 1962. Ion exchange. MacGraw-Hill Book Company, Inc., New York.

36. Helfferich, F., and M. S. Plesset. 1957. Ion exchange kinetics. A non-linear diffusion problem. J. Chem. Phys. 28:418-424.

37. Jenny, H. 1932. Studies on the mechanism of ionic exchange on colloidal aluminum silicates. J. Phys. Chem. 36:2217-2258.

38. Jenny, H. 1936. Simple kinetic theory of ion exchange I. Ions of equal valence. J. Phys. Chem. 40:501-517.

39. Jost, W. 1952. Diffusion in solids, liquids and gases. Chap. 1- The fundamental laws of diffusion. Academic Press, New York.

40. Kasten, P. R., L. Lapidus, and N. R. Amundson. 1952. Mathematics of adsorption in beds V. Effect of intra-particle diffusion in flow systems in fixed beds. J. Phys. Chem. 56:683-688.

41. Kelley, W. P., and H. Jenny. 1936. The relation of crystal structure to base exchange and its bearing to base exchange in soil. Soil Sci. 41:367-382.

42. Kerr, H. W. 1928. The nature of base exchange and soil acidity. J. Amer. Soc. Agron. 20:309-335.

43. Kielland, J. 1937. Individual activity coefficients of ions in aqueous solutions. J. Amer. Chem. Soc. 59:1675-1678.

44. Kressman, R. E., and J. A. Kitchener. 1949. Cation exchange with a synthetic phenolsulphonate resin part V. Kinetics. Disc. Faraday Soc. 7:90-104.

45. Lai, Sung-Ho. 1970. Cation exchange and transport in soil columns undergoing miscible displacement. Ph.D. dissertation, Utah State Univ., Logan, Utah.

46. Lindstrom, F. T., R. Haque, V. H. Freed, and L. Boersma. 1967. Theory on the movement of some herbicides in soils. Linear diffusion and convection of chemicals in soils. Env. Sci. and Tech. 1:561-565.

47. Mattson, S., and K. G. Larsson. 1946. The laws of soil colloidal behaviour XXIV. Donnan equilibria in soil formation. Soil Sci. 61:313-330.

48. Meyers, R. J., J. W. Eastes, and F. J. Meyers. 1941. Synthetic resins as exchange absorbents. Ind. Eng. Chem. 33:697-706.

49. Millar, J. R., D. G. Smith, W. E. Marr, and T. R. E. Kressman. 1963. Solvent-modified polymer networks. Part 1. The preparation and characterization of expanded network and macroporous styrene-divinylbenzene copolymers and their sulphonates. J. Chem. Soc. 116 part 1:218-225.

50. Millar, J. R., D. G. Smith, W. E. Marr, and T. R. E. Kressman. 1963. Solvent-modified polymer networks. Part 2. Effect of structure on cation exchange kinetics in sulphonated styrene divinylbenzene copolymers. J. Chem. Soc. 116:2779-2784.

51. Mills, R. 1973. Self-diffusion in normal and heavy water in the range 1 - 45 C. J. Phys. Chem. 77:685-688.

52. Nielsen, D. R., and J. W. Biggar. 1961. Miscible displacement in soils I. Experimental information. Soil Sci. Soc. Amer. Proc. 25:1-5.

53. Nielsen, D. R., and J. W. Biggar. 1962. Miscible displacement III. Theoretical considerations. Soil Sci. Soc. Amer. Proc. 26:216-221.

54. Nir, A., and N. D. Gershon. 1969. Effects of boundary conditions on models of tracer distribution in flow through porous media. Water Resources Res. 5:830-839.

55. Pinder, G. F., and W. G. Gray. 1977. Finite element simulation in surface and subsurface hydrology. Academic Press, New York.

56. Plesset, M. S., F. Helfferich, and J. N. Franklin. 1958. Ion exchange kinetics. A non-linear diffusion problem II. Particle diffusion controlled exchange of univalent and bivalent ions. J. Chem. Phys. 29:1064-1069.

57. Rachinskii, V. V. 1965. The general theory of sorption dynamics and chromatography. Translation from Russian. Consultants Bureau, New York.

58. Reichenberg, D. 1953. Properties of ion exchange resins in relation to their structure III. Kinetics of exchange. J. Amer. Chem. Soc. 75:589-597.

59. Rifai, M. N. E., W. J. Kaufman, and D. W. Todd. 1956. Dispersion phenomena in laminar flow through porous media. Sanitary Eng. Res. Lab., Univ. of Calif., Berkeley, Progress Rept. No. 2.

60. Roberts, G. E., and H. Kaufman. 1966. Table of Laplace transforms- p. 255. W. B. Saunders Co., Philadelphia and London.

61. Rose, D. A., and J. B. Passioura. 1971. The analysis of experiments on hydrodynamic dispersion. Soil Sci. 111:252-257.

62. Rose, D. A., and J. B. Passioura. 1971. Gravity segregation during miscible displacement experiments. Soil Sci. 111:258-265.

63. Rosen, J. B. 1952. Kinetics of a fixed bed system for solid diffusion into spherical particles. J. Chem. Phys. 20:387-394.

64. Saffman, P. G. 1959. A theory of dispersion in a porous medium. J. Fluid Mech. 6:321-349.

65. Scheidegger, A. E. 1954. Statistical hydrodynamics in porous media. J. Appl. Phys. 25:997-1001.

66. Scheidegger, A. E. 1960. The physics of flow through porous media. 2nd. ed. Univ. of Toronto Press.

67. Taylor, G. I. 1953. Dispersion of soluble matter in solvent flowing slowly through a tube. Proc. Roy. Soc. London A 219:186-203.

68. Van Deemter, J. J., F. J. Zuiderweg, and A. Klinkenberg. 1956. Longitudinal diffusion and resistance to mass transfer as causes of nonideality in chromatography. Chem. Eng. Sci. 5:271-289.

69. Van Genuchten, T. M. 1974. Mass transfer studies in sorbing porous media. Ph.D. dissertation, New Mexico State Univ., Las Cruces, New Mexico.

70. Van Genuchten, T. M., J. M. Davidson, and P. J. Wierenga. 1973. An evaluation of kinetic and equilibrium equations for the prediction of pesticide movement through porous media. Soil Sci. Soc. Amer. Proc. 38:29-35.

71. Van Olphen, H. 1963. An introduction to clay colloid chemistry. Interscience Publishers, New York.

72. Vanselow, A. P. 1932. Equilibria of the base exchange reactions of bentonites, permutites, soil colloids and zeolites. Soil Sci. 33:95-113.

73. Way, J. T. 1850. On the power of soils to absorb manure. Jour. Roy. Agric. Soc. England 11:313-379.

74. Way, J. T. 1852. On the power of soils to absorb manure. Jour. Roy. Agric. Soc. England 13:123-143.

75. Wehner, J. F., and R. H. Wilhelm. 1956. Boundary conditions of flow reactor. Chem. Eng. Sci. 6:89-93.

BIOGRAPHICAL SKETCH

NARAINE PERSAUD was born on July 2, 1944, in GUYANA, South America. He completed his secondary education at Queen's College, Georgetown, GUYANA, in 1962. Two years later he entered the Agricultural Institute, Allahabad, India, and in 1968 he obtained his BSc. degree in agriculture with specialisation in animal husbandry and dairying. Subsequently, he served for one year as lecturer at the School of Agriculture, Monrepos, GUYANA, and thereafter as an extension officer in the Ministry of Agriculture in GUYANA. In September 1974 he entered the University of Florida where he obtained his MSc. degree in horticulture in March 1976. Immediately thereafter, he began work in the soil science department of the same university toward his PhD. degree for which he is currently a candidate. He is married to the former Savitri Singh and is the father of two children Salendra and Nalendra.

I certify that I have read this study and that in my opinion it conforms to acceptable standards of scholarly presentation and is fully adequate, in scope and quality, as a dissertation for the degree of Doctor of Philosophy.

James M. Davidson, Chairman
Professor of Soil Science

I certify that I have read this study and that in my opinion it conforms to acceptable standards of scholarly presentation and is fully adequate, in scope and quality, as a dissertation for the degree of Doctor of Philosophy.

John G. A. Fiskell
Professor of Soil Science

I certify that I have read this study and that in my opinion it conforms to acceptable standards of scholarly presentation and is fully adequate, in scope and quality, as a dissertation for the degree of Doctor of Philosophy.

L. Hammond
Professor of Soil Science

I certify that I have read this study and that in my opinion it conforms to acceptable standards of scholarly presentation and is fully adequate, in scope and quality, as a dissertation for the degree of Doctor of Philosophy.

Salvadore J. Locascio
Professor of Horticulture

This dissertation was submitted to the Graduate Faculty of the College of Agriculture and to the Graduate Council, and was accepted as partial fulfillment of the requirements for the degree of Doctor of Philosophy.

June, 1978

Dean, College of Agriculture

Dean, Graduate School